Latest Development in Inorganic Scintillators and Readout for Future Crystal Calorimeters

Ren-Yuan Zhu

California Institute of Technology

July 22, 2020

Presentation in the Online Mini-Workshop on a Crystal ECAL

Why Crystal Calorimetry?

- Precision photons and electrons measurements enhance physics discovery potential in HEP experiments.
- Performance of crystal calorimeter is well understood for e/γ, and is investigated for jets measurements :
  - The best possible energy resolution and position resolution;
  - Good e/γ identification and reconstruction efficiency;
  - Excellent jet mass resolution with dual readout, either C/S and F/S gate.
- Novel Inorganic Scintillators for Future HEP experiments:
  - Bright, fast and rad-hard for HL-LHC and FCC-hh: LYSO and LuAG ceramics;
  - Ultrafast for high rate, e.g. Mu2e-II, and ultrafast timing: BaF_2:Y;
  - Cost-effective crystals for homogeneous hadron calorimetry: Sapphire:Ti.

Existing Crystal Calorimeters in HEP

Date	75-85	80-00	80-00	80-00	90-10	94-10	94-10	95-Now	10-Now
Experiment	C. Ball	L3	CLEO II	C. Barrel	KTeV	BaBar	BELLE	CMS	BES III
Accelerator	SPEAR	LEP	CESR	LEAR	Tevatron	PEP	KEKB	LHC	BEPC
Laboratory	SLAC	CERN	Cornell	CERN	FNAL	SLAC	KEK	CERN	IHEP
Crystal Type	NaI:Tl	BGO	CsI:Tl	CsI:Tl	CsI	CsI:Tl	CsI:Tl	PWO	CsI:Tl
B-Field（T）	-	0.5	1.5	1.5	-	1.5	1.0	4.0	1.0
r_{inner} (m)	0.254	0.55	1.0	0.27	-	1.0	1.25	1.29	0.94
Crystal number	672	11,400	7,800	1,400	3,300	6,580	8,800	75,848	6,240
Crystal Depth（X_0）	16	22	16	16	27	16 to 17.5	16.2	25	15
Crystal Volume（m^3）	1	1.5	7	1	2	5.9	9.5	11	5.3
Light Output（p.e./MeV）	350	1,400	5,000	2,000	40	5,000	5,000	2	5,000
Photo-detector	PMT	Si PD	Si PD	WS+Si PD	PMT	Si PD	Si PD	Si APD	Si PD
Gain of Photo-detector	Large	1	1	1	4,000	1	1	50	1
σ_N/Channel（MeV）	0.05	0.8	0.5	0.2	Small	0.15	0.2	40	0.2
Dynamic Range	10^4	10^5	10^4	10^4	10^4	10^4	10^4	10^5	10^4

Crystals with Mass Production Capability

Crystal	NaI:Tl	CsI:Tl	CsI	BaF_2	CeF_3	PbF_2	BGO	BSO	$PbWO_4$	LYSO:Ce	AFO Glasses	Sapphire:Ti
Density (g/cm^3)	3.67	4.51	4.51	4.89	6.16	7.77	7.13	6.8	8.3	7.40	4.6	3.98
Melting points (^oC)	651	621	621	1280	1460	824	1050	1030	1123	2050	-	2040
X_0 (cm)	2.59	1.86	1.86	2.03	1.65	0.94	1.12	1.15	0.89	1.14	2.96	7.02
R_M (cm)	4.13	3.57	3.57	3.10	2.39	2.18	2.23	2.33	2.00	2.07	2.89	2.88
λ_I (cm)	42.9	39.3	39.3	30.7	23.2	22.4	22.7	23.4	20.7	20.9	26.4	24.2
Z_{eff}	50.1	54.0	54.0	51.6	51.7	77.4	72.9	75.3	74.5	64.8	42.8	11.2
dE/dX (MeV/cm)	4.79	5.56	5.56	6.52	8.40	9.42	8.99	8.59	10.1	9.55	6.84	6.75
λ_{peak} [a] (nm)	410	560	420 310	300 220	340 300	\	480	470	425 420	420	365	300 750
Refractive Index[b]	1.85	1.79	1.95	1.50	1.62	1.82	2.15	2.68	2.20	1.82	-	1.76
Normalized Light Yield[a,c]	120	190	4.2 1.3	42 4.8	8.6	\	25	5	0.4 0.1	**100**	1.5	0.04 0.22
Total Light yield (ph/MeV)	35,000	58,000	1700	13,000	2,600	\	7,400	1,500	130	30,000	450	7,900
Decay time[a] (ns)	245	1220	30 6	600 0.5	30	\	300	100	30 10	40	40	300 3200
Hygroscopic	Yes	Slight	Slight	No	No	No	No	No	No	No	No	No
Experiment	Crystal Ball	CLEO BaBar BELLE BES III	KTeV Mu2e	TAPS	-	A4 g-2	L3 BELLE	-	CMS ALICE PrimEx Panda	CMS BTL COMET HERD	-	HHCAL?

DOE Basic Research Needs Study on Instrumentation: Calorimetry

Priority Research Direction
PRD 1: Enhance calorimetry energy resolution for precision electroweak mass and missing-energy measurements
PRD 2: Advance calorimetry with spatial and timing resolution and radiation hardness to master high-rate environments
PRD 3: Develop ultrafast media to improve background rejection in calorimeters and improve particle identification

Energy, spatial and timing resolution, and radiation hard and ultrafast media

Fast and Ultrafast Inorganic Scintillators

	BaF_2	BaF_2:Y	ZnO:Ga	YAP:Yb	YAG:Yb	β-Ga_2O_3	LYSO:Ce	LuAG:Ce	YAP:Ce	GAGG:Ce	LuYAP:Ce	YSO:Ce
Density (g/cm^3)	4.89	4.89	5.67	5.35	4.56	5.94[1]	7.4	6.76	5.35	6.5	7.2[f]	4.44
Melting points (°C)	1280	1280	1975	1870	1940	1725	2050	2060	1870	1850	1930	2070
X_0 (cm)	2.03	2.03	2.51	2.77	3.53	2.51	1.14	1.45	2.77	1.63	1.37	3.10
R_M (cm)	3.1	3.1	2.28	2.4	2.76	2.20	2.07	2.15	2.4	2.20	2.01	2.93
λ_I (cm)	30.7	30.7	22.2	22.4	25.2	20.9	20.9	20.6	22.4	21.5	19.5	27.8
Z_{eff}	51.6	51.6	27.7	31.9	30	28.1	64.8	60.3	31.9	51.8	58.6	33.3
dE/dX (MeV/cm)	6.52	6.52	8.42	8.05	7.01	8.82	9.55	9.22	8.05	8.96	9.82	6.57
λ_{peak}[a] (nm)	300 220	300 220	380	350	350	380	420	520	370	540	385	420
Refractive Index[b]	1.50	1.50	2.1	1.96	1.87	1.97	1.82	1.84	1.96	1.92	1.94	1.78
Normalized Light Yield[a,c]	42 4.8	1.7 4.8	6.6[d]	0.19[d]	0.36[d]	6.5 0.5	100	35[e] 48[e]	9 32	115	16 15	80
Total Light yield (ph/MeV)	13,000	2,000	2,000[d]	57[d]	110[d]	2,100	30,000	25,000[e]	12,000	34,400	10,000	24,000
Decay time[a] (ns)	600 0.5	600 0.5	<1	1.5	4	148 6	40	820 50	191 25	800 80	1485 36	75
LY in 1st ns (photons/MeV)	1200	1200	610[d]	28[d]	24[d]	43	740	240	391	640	125	318
40 keV Att. Leng. (1/e, mm)	0.106	0.106	0.407	0.314	0.439	0.394	0.185	0.251	0.314	0.319	0.214	0.334

Applications in HEP Experiments

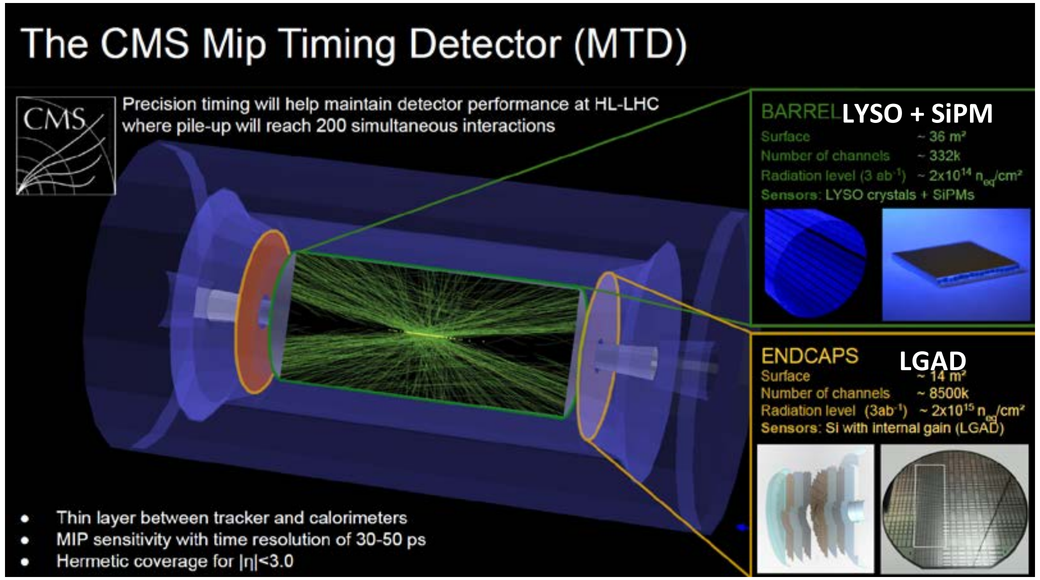

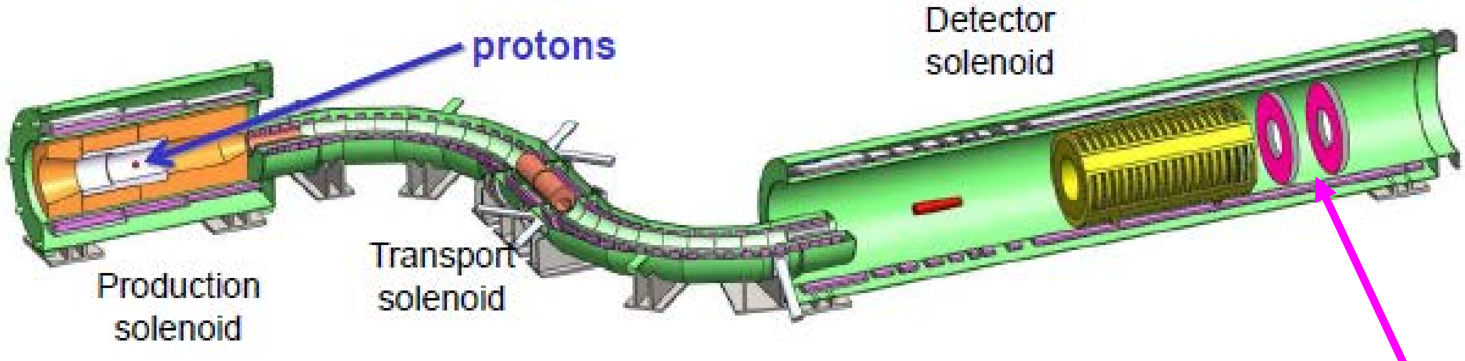

Mu2e-II: arXiv:1802.02599

Mu2e-I: 1,348 CsI of 34 x 34 x 200 mm
Mu2e-II: 1,940 BaF_2:Y of 30 x 30 x 218 mm

2%/√E ⊕ 0.5%

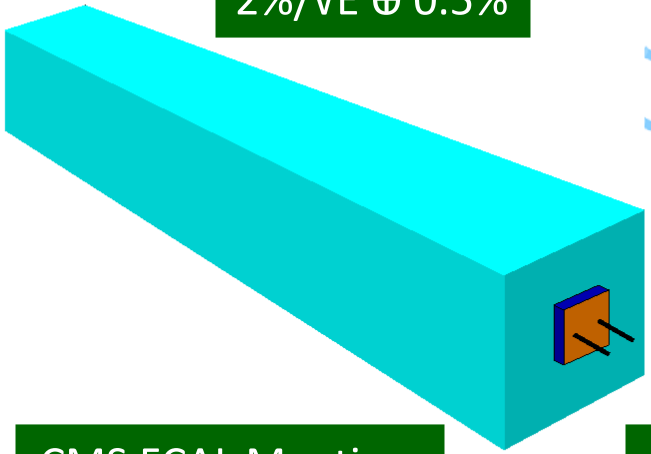

CMS FCAL Meeting at CERN, 6/30/2011

10%/√E ⊕ 1%

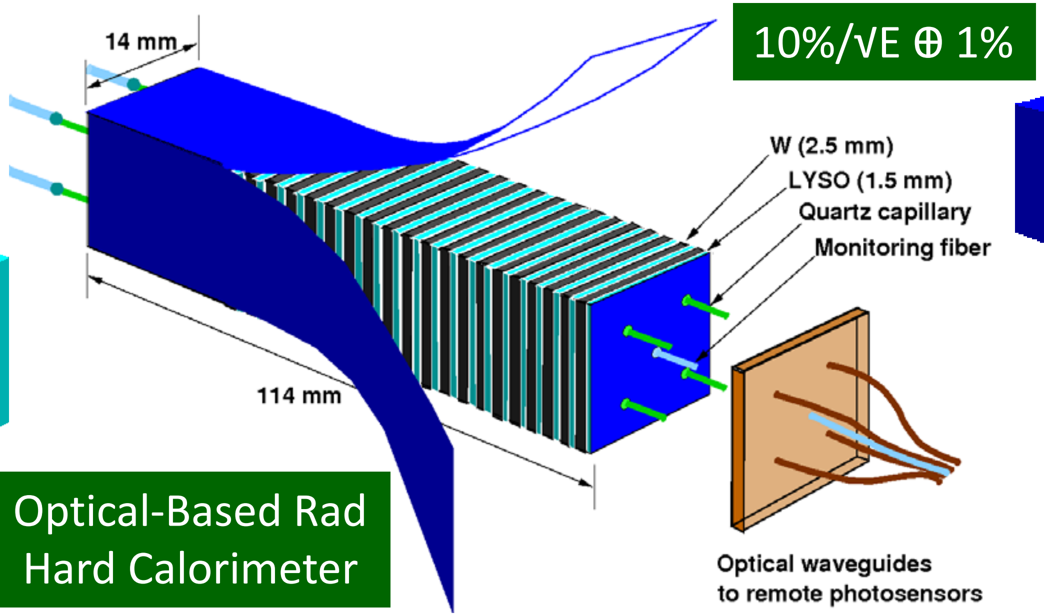

Optical-Based Rad Hard Calorimeter

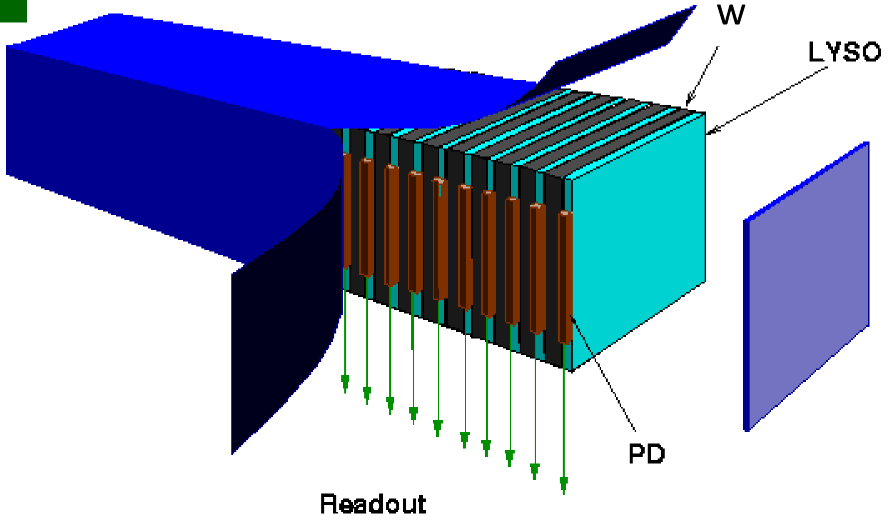

CMS MTD: Expected Radiation

CMS MTD/FCAL: 4.8/68 Mrad, $2.5\times10^{13}/2.1\times10^{14}$ p/cm^2 & $3.2\times10^{14}/2.4\times10^{15}$ n_{eq}/cm^2

CMS MTD	η	n_{eq} (cm^{-2})	n_{eq} Flux ($cm^{-2}s^{-1}$)	Protons (cm^{-2})	p Flux ($cm^{-2}s^{-1}$)	Dose (Mrad)	Dose rate (rad/h)
Barrel	0.00	2.48E+14	2.75E+06	2.2E+13	2.4E+05	2.7	108
Barrel	1.15	2.70E+14	3.00E+06	2.4E+13	2.6E+05	3.8	150
Barrel	**1.45**	**2.85E+14**	**3.17E+06**	**2.5E+13**	**2.8E+05**	**4.8**	**192**
Endcap	1.60	2.3E+14	2.50E+06	2.0E+13	2.2E+05	2.9	114
Endcap	2.00	4.5E+14	5.00E+06	3.9E+13	4.4E+05	7.5	300
Endcap	2.50	1.1E+15	1.25E+07	9.9E+13	1.1E+06	25.5	1020
Endcap	**3.00**	**2.4E+15**	**2.67E+07**	**2.1E+14**	**2.3E+06**	**67.5**	**2700**

More than three orders of magnitude at FCC-hh: **500 Grad and 5×10^{18} n_{eq}/cm^2**

Particle Spectra at HL-LHC

FLUKA simulations: neutrons and charged hadrons peaked at MeV and several hundreds MeV, respectively. Neutron and proton induced damages were investigated at the East Port and the Blue Room of the Los Alamos Neutron Science Center (LANSCE), respectively

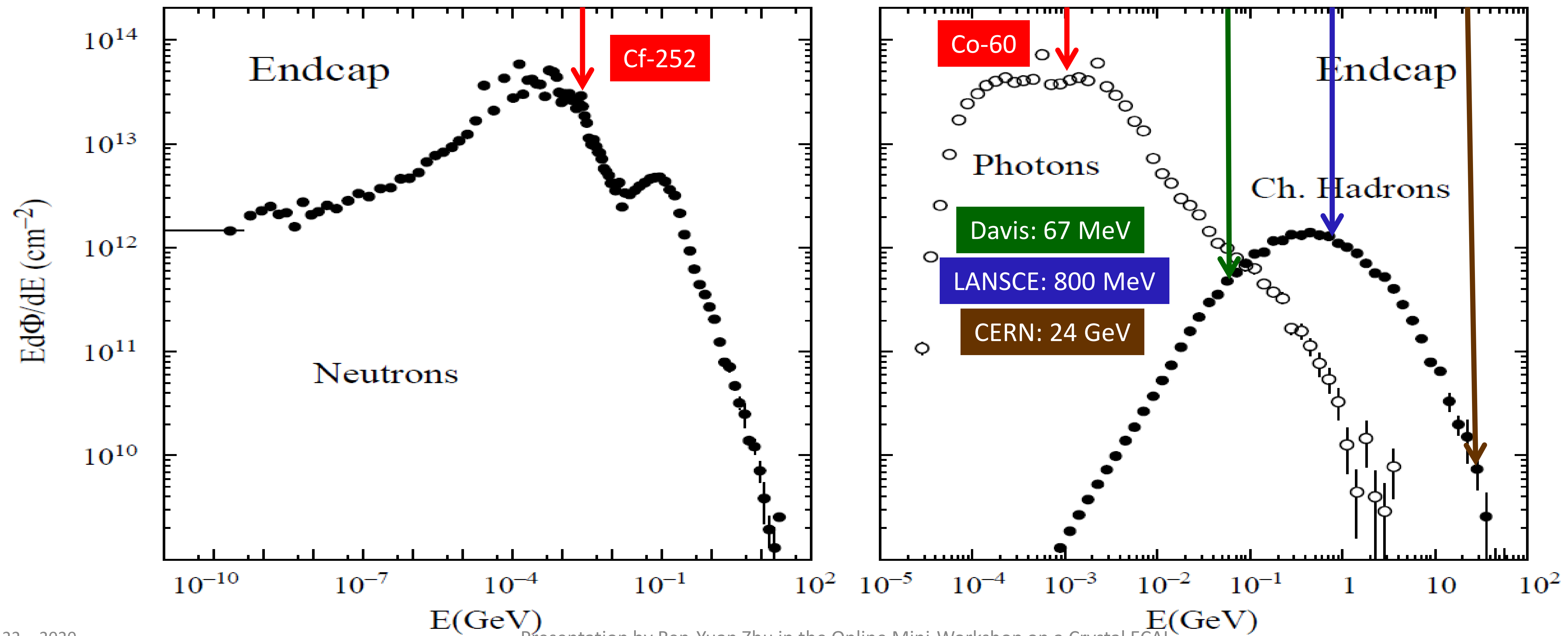

Hadron Irradiation at LANSCE

Irradiation by 800 MeV protons in three experiments 6501, 6990 and 7324 up to 3 x 10^{15} p/cm^2 was carried out at the target 2 in the blue room of LANSCE, where crystals and shashlik calorimeter towers were measured *in situ* by a home-made spectrophotometer.

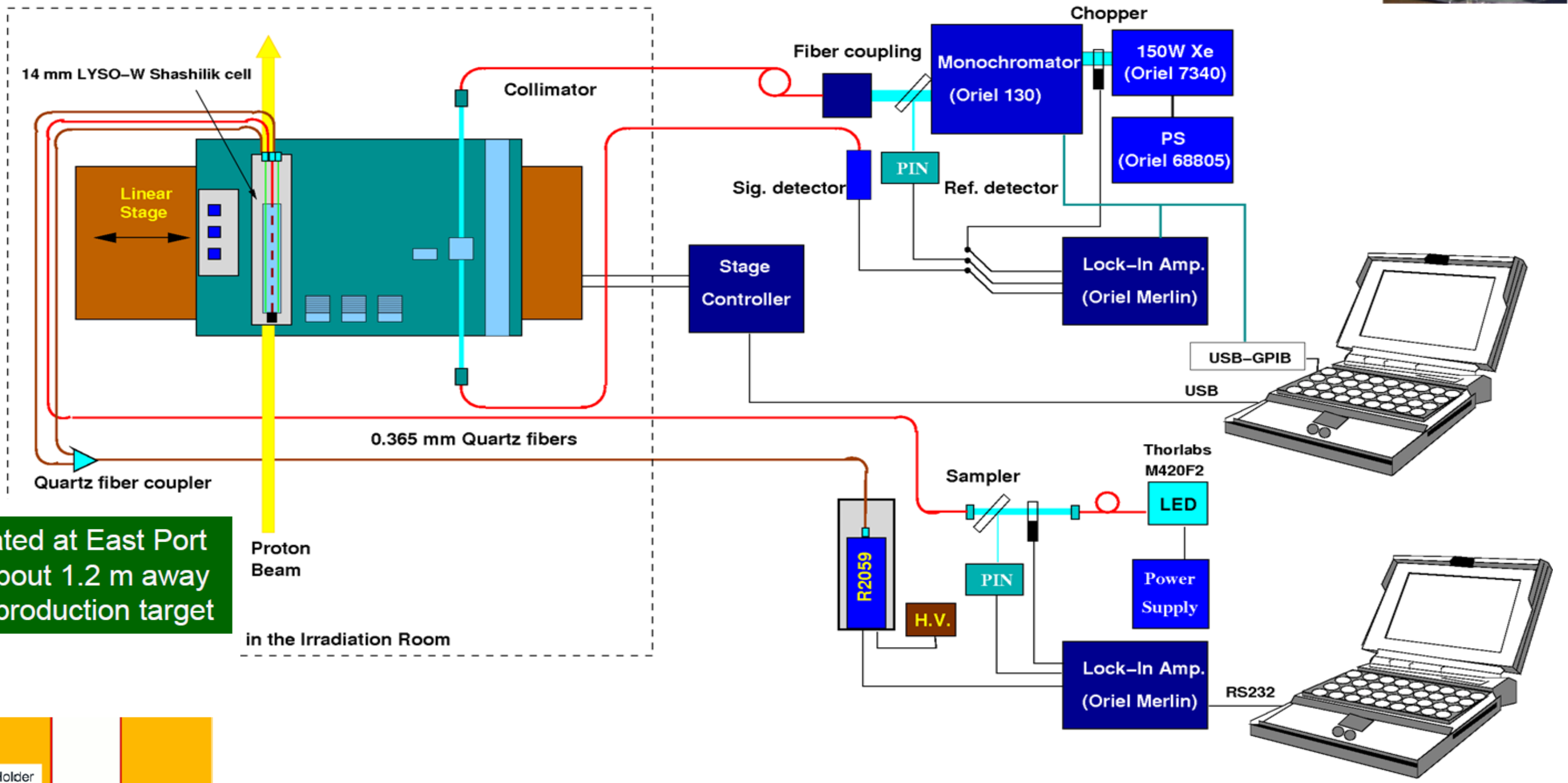

Los Alamos Neutron Science Center (LANSCE)

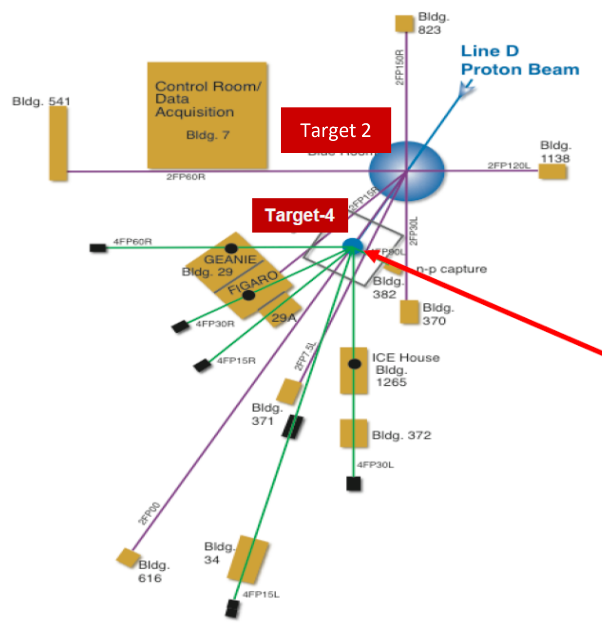

Samples are located at East Port in the Target-4, about 1.2 m away from the neutron production target

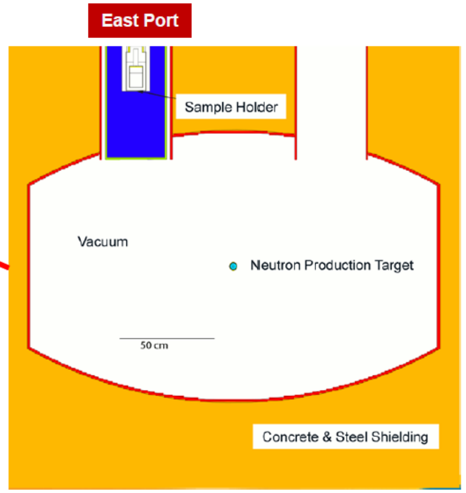

Irradiation by neutrons in three experiments 6991, 7332 and 7638 up to 3 x 10^{15} n_{eq}/cm^2 at the target 4 in the East Port of LANSCE with 1 MeV equivalent neutron flux calculated by using MCNPX (Monte Carlo N-Particle eXtended) package tallied in the largest sample volume (averaging).

LYSO Radiation Hardness

CMS BTL spec: < 3 m^{-1} after 4.8 Mrad, 2.5 x 10^{13} p/cm^2 and 3.2 x 10^{14} n_{eq}/cm^2

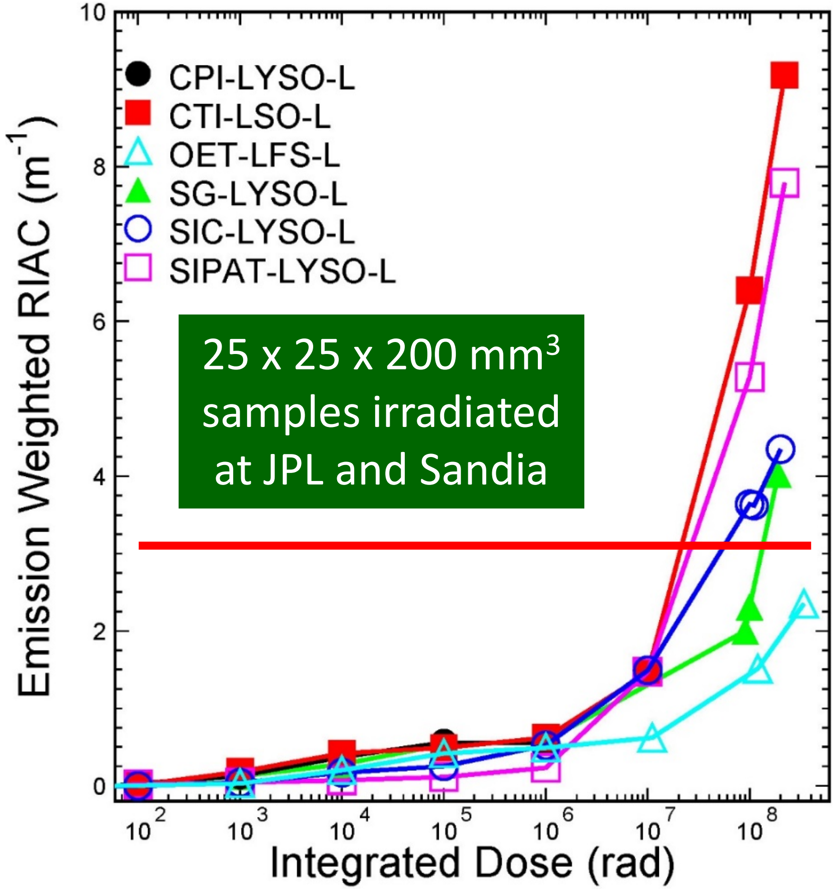

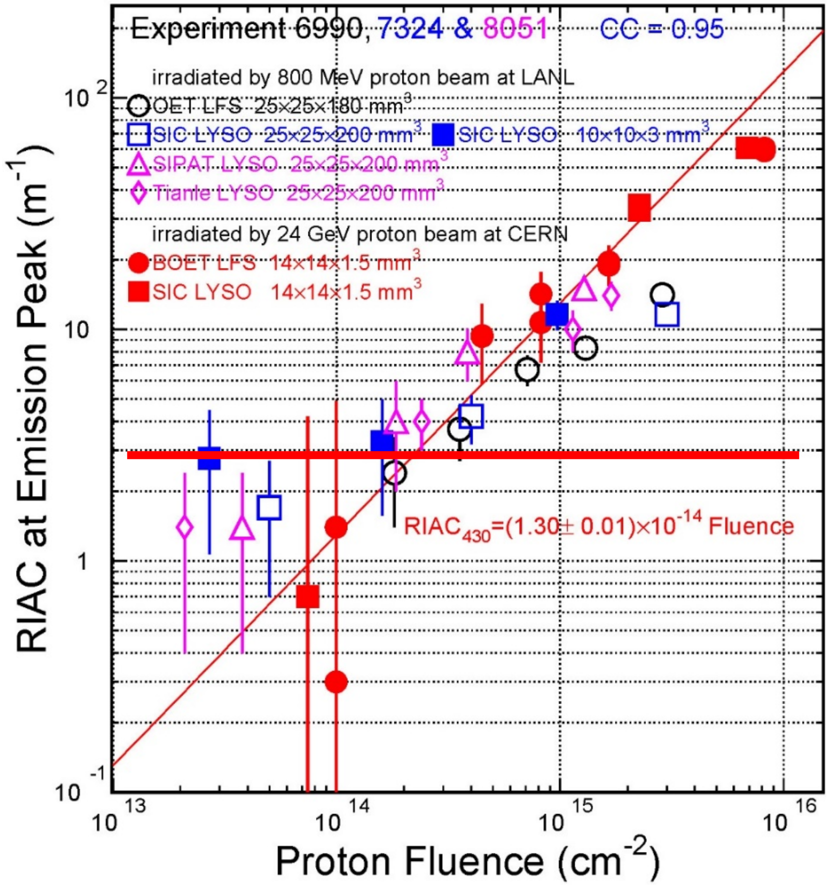

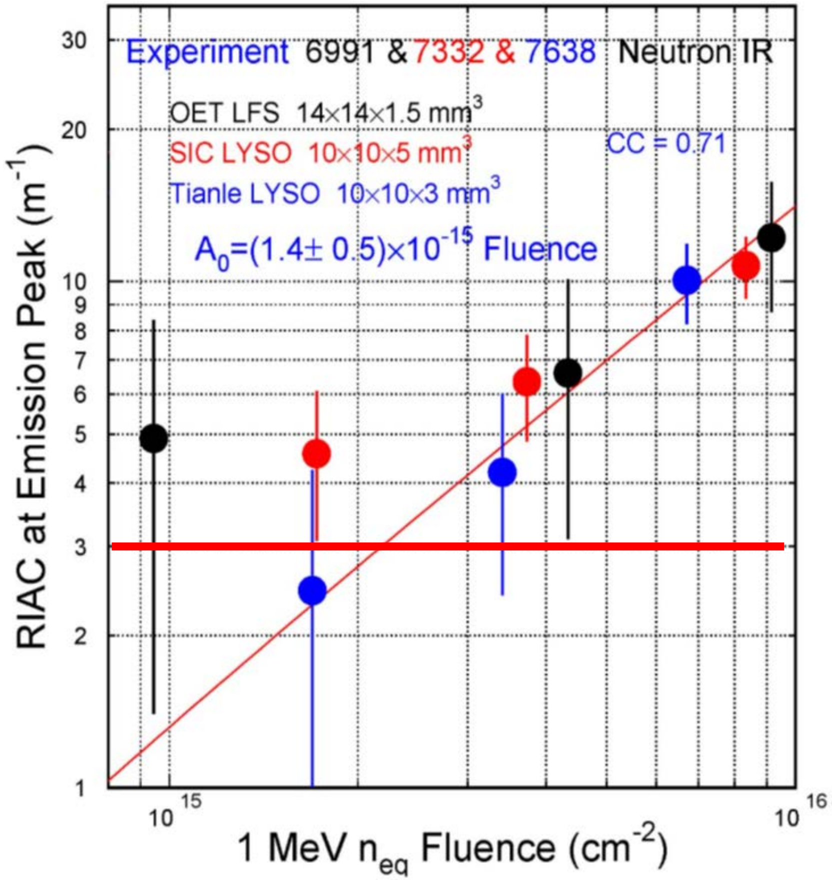

Damage induced by protons is an order of magnitude larger than that from neutrons
Presumably due to ionization energy loss in addition to displacement and nuclear breakup

Radiation Induced Readout Noise

Radiation induced readout noise (~30 keV) was determined by measuring the radiation induced photo-current in LYSO+SiPM under the expected dose rate and neutron fluence

$$F = \frac{\frac{Photocurrent}{Charge_{electron} \times Gain_{SiPM}}}{Dose\ rate_{\gamma-ray}\ or\ Flux_{neutron}} \qquad \sigma = \frac{\sqrt{Q}}{LO} \quad \text{(MeV)}$$

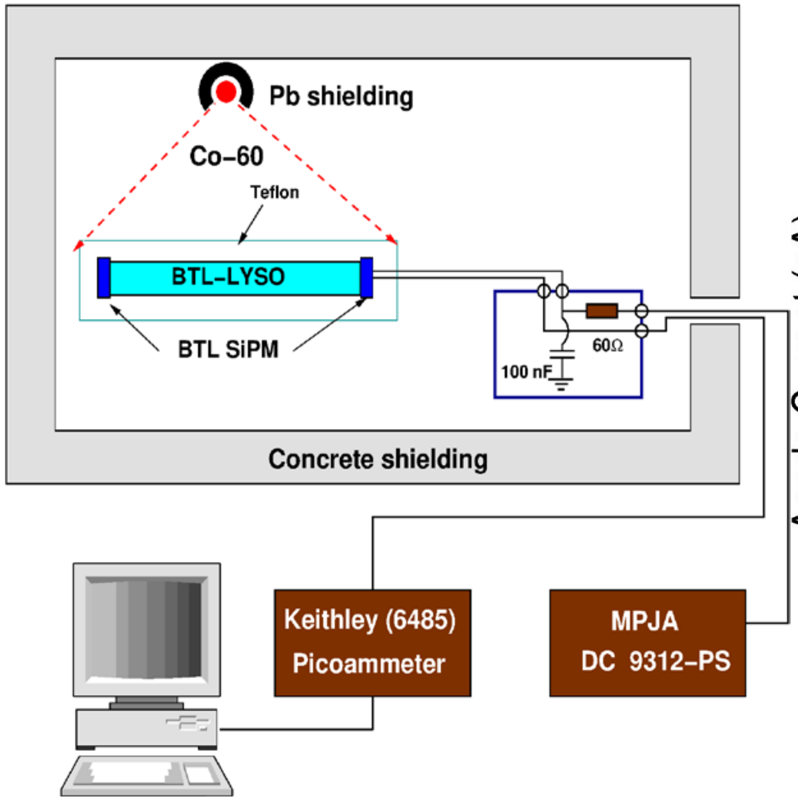

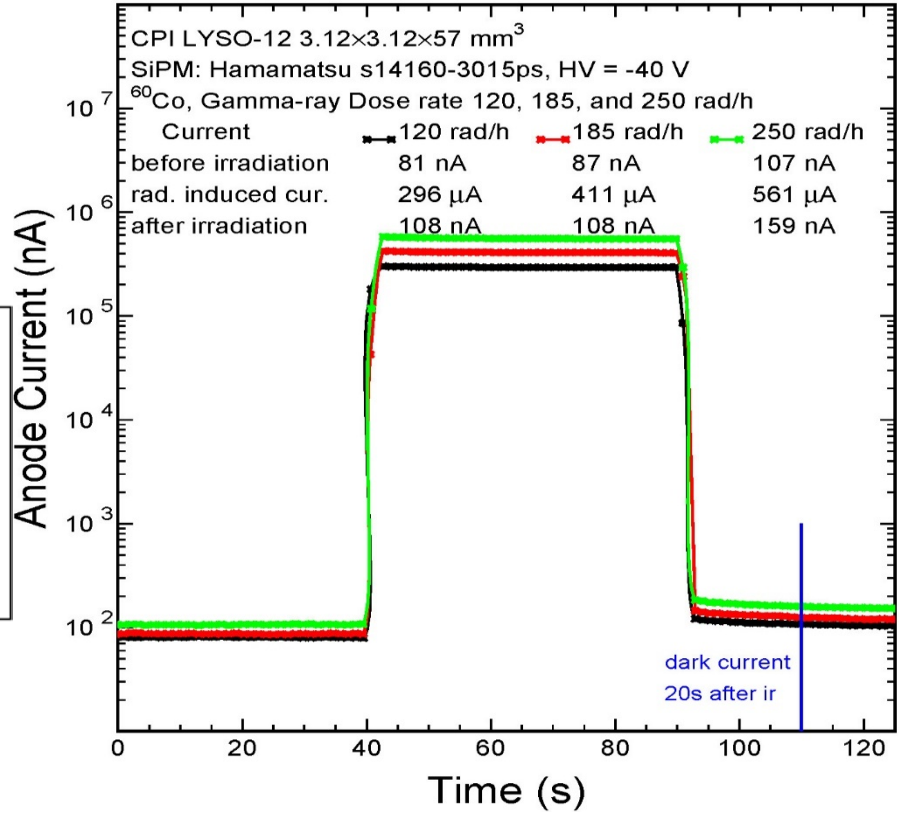

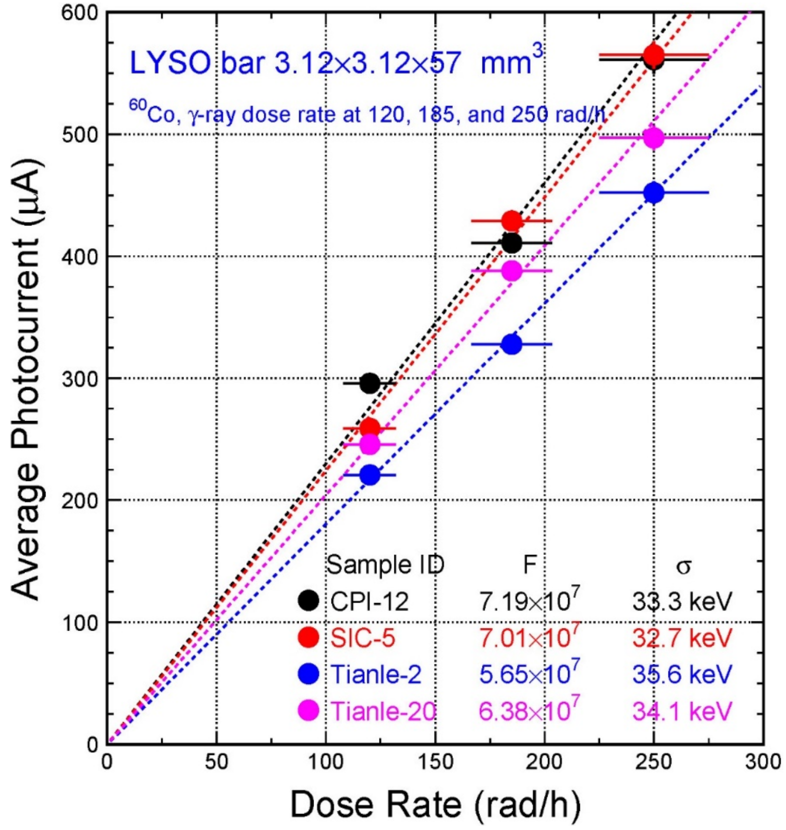

LuAG:Ce Ceramic Samples

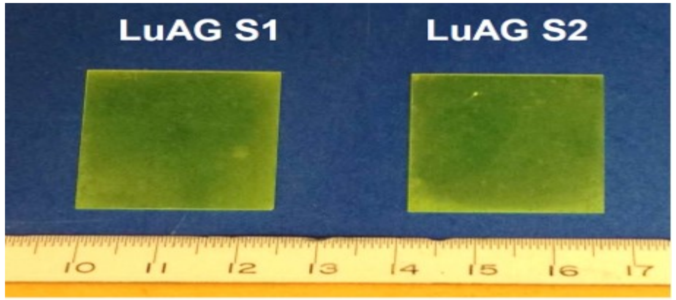

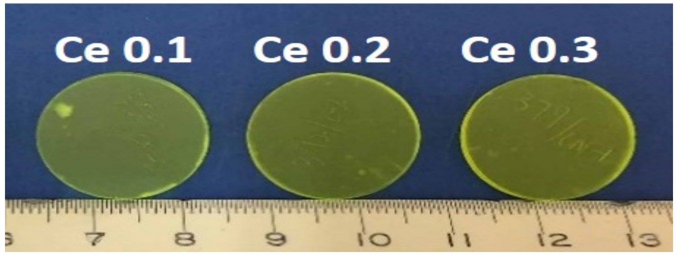

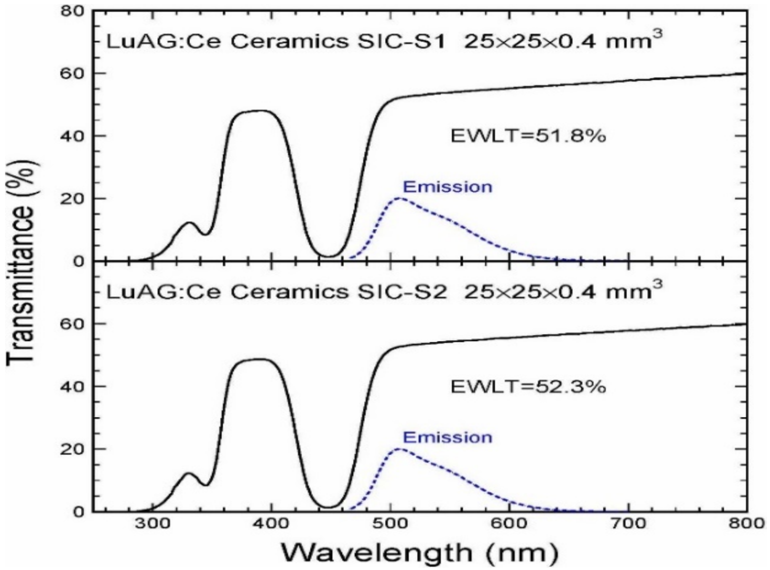

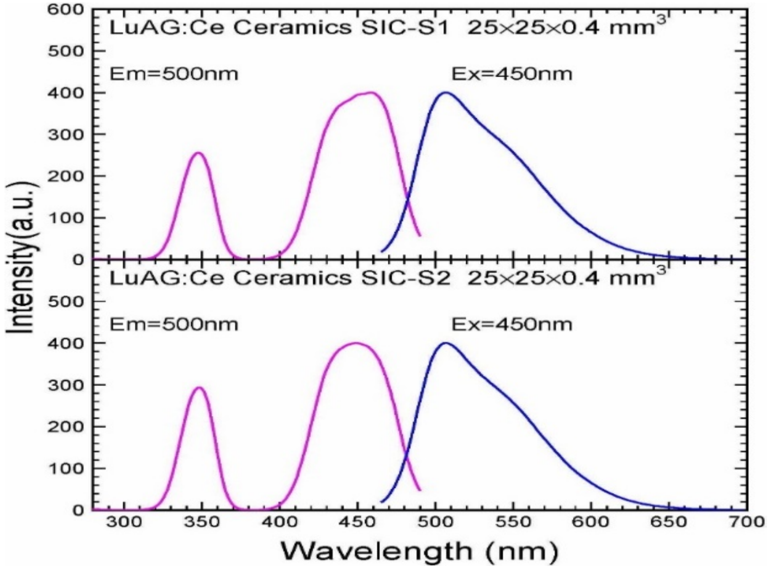

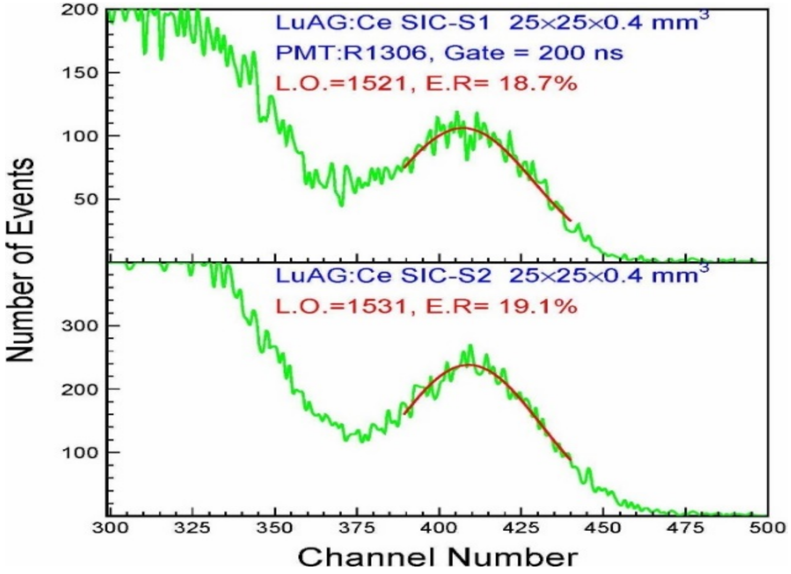

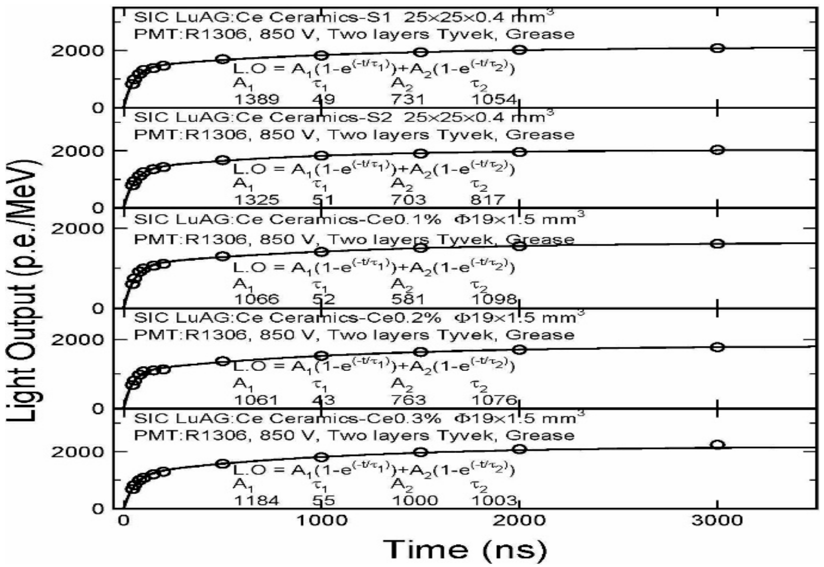

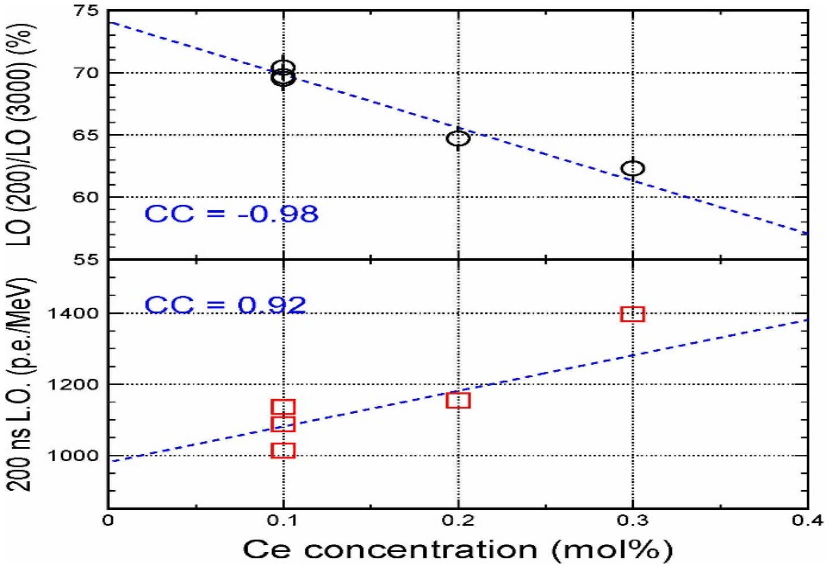

Radiation Hard LuAG:Ce Ceramics

Rad-hard up to 3×10¹⁴ p/cm² and 220 Mrad: promising for FCC-hh

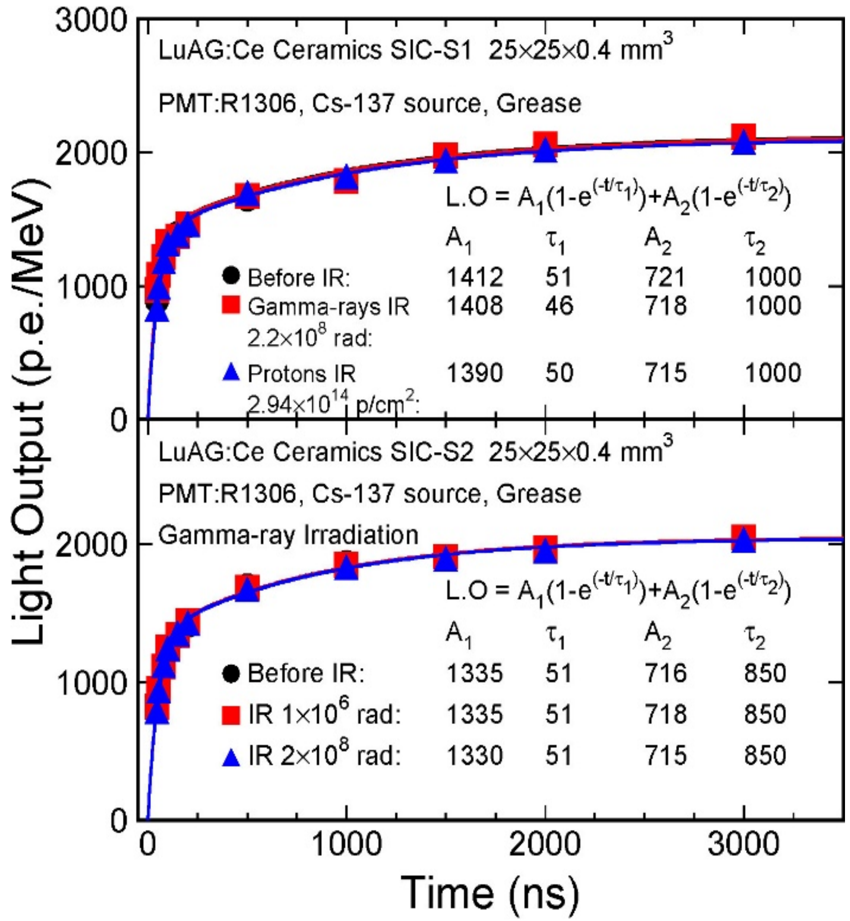

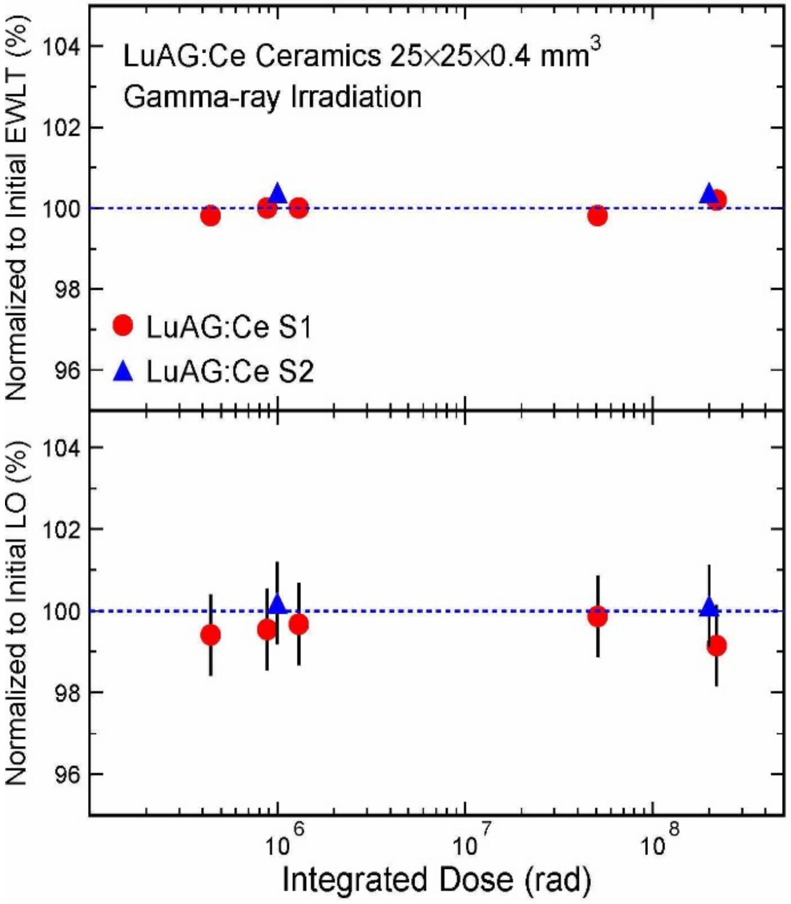

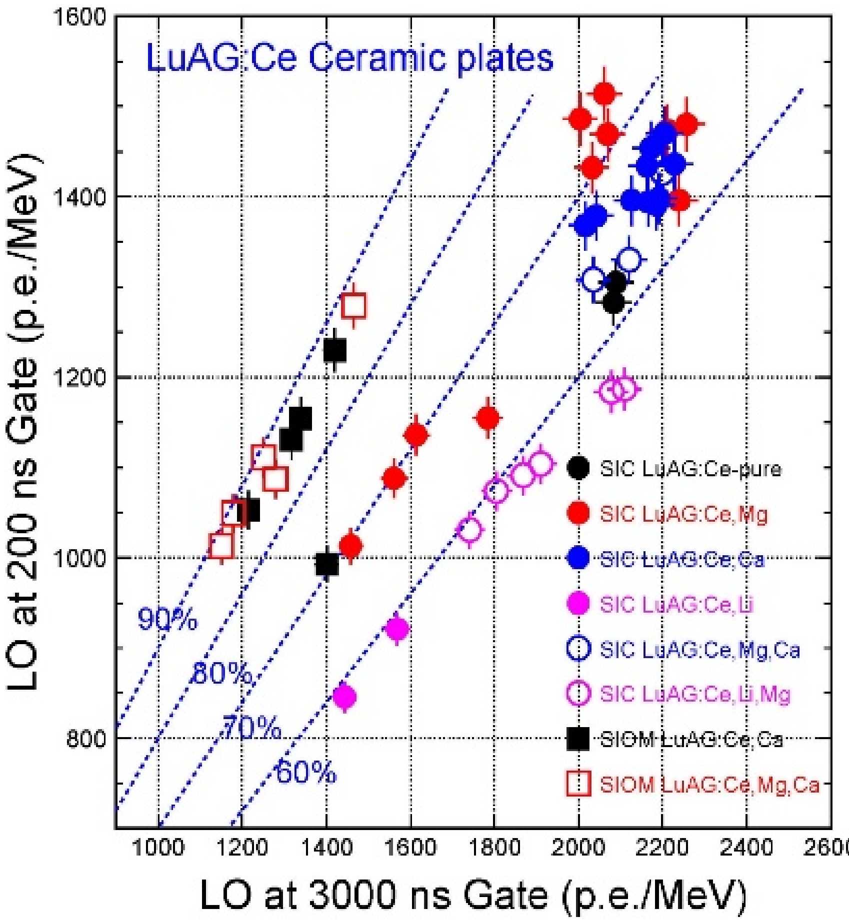

R&D on slow component suppression by Pr doping or co-doping

Ultrafast and Slow Light from BaF_2

BaF_2 has a ultrafast scintillation component @ 220 nm with 0.5 ns decay time and an intensity a little less than undoped CsI. It has also a factor of 5 larger slow component @ 300 nm with 300 ns decay time.

Slow suppression may be achieved by selective rare earth doping, e.g. Y, La and Ce, in BaF_2, and/or photodetectors with filters or a solar- blind cathode, e.g. Cs-Te, K-Cs-Te and Rb-Te.

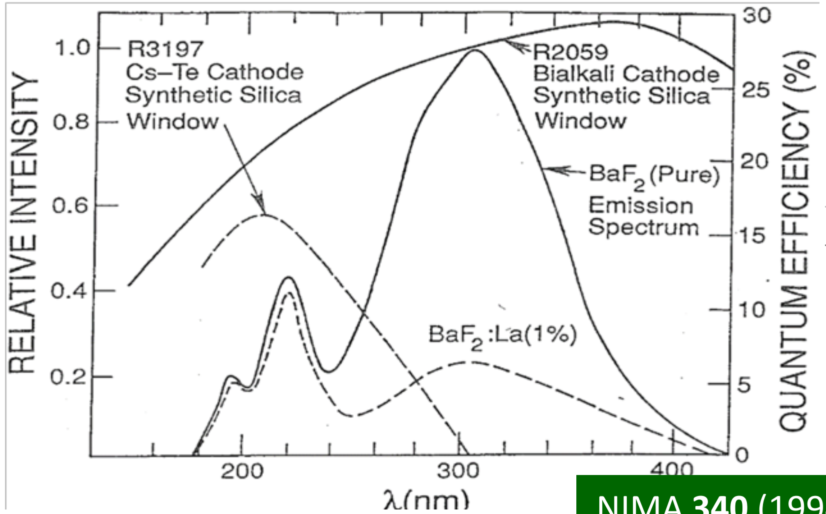

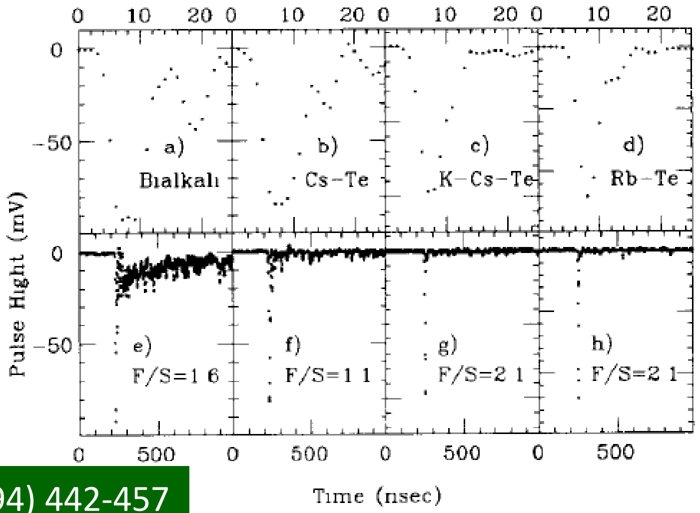

NIMA **340** (1994) 442-457

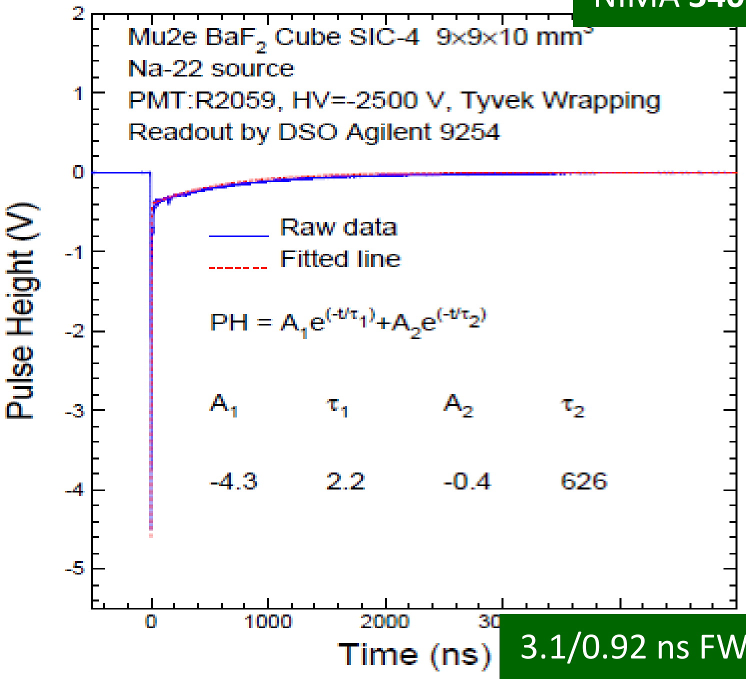

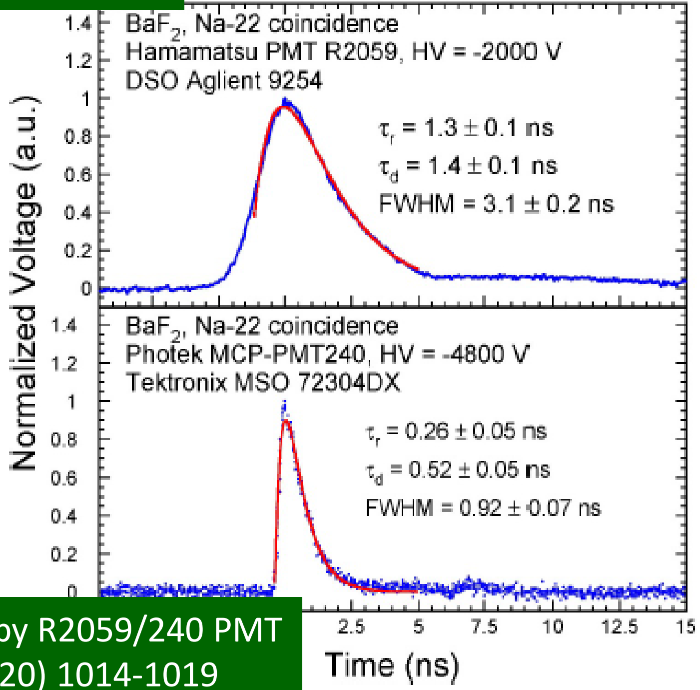

3.1/0.92 ns FWHM by R2059/240 PMT
IEEE TNS **67** (2020) 1014-1019

Slow Suppression: Doping & Readout

Slow suppression by RE doped BaF_2 powders: Y, La and Ce (1994)

B.P. SOBOLEV et al., "SUPPRESSION OF BaF2 SLOW COMPONENT OF X-RAY LUMINESCENCE IN NON-STOICHIOMETRIC Ba0.9R0.1F2 CRYSTALS (R=RARE EARTH ELEMENT)," *Proceedings of The Material Research Society: Scintillator and Phosphor Materials*, pp. 277-283, 1994.

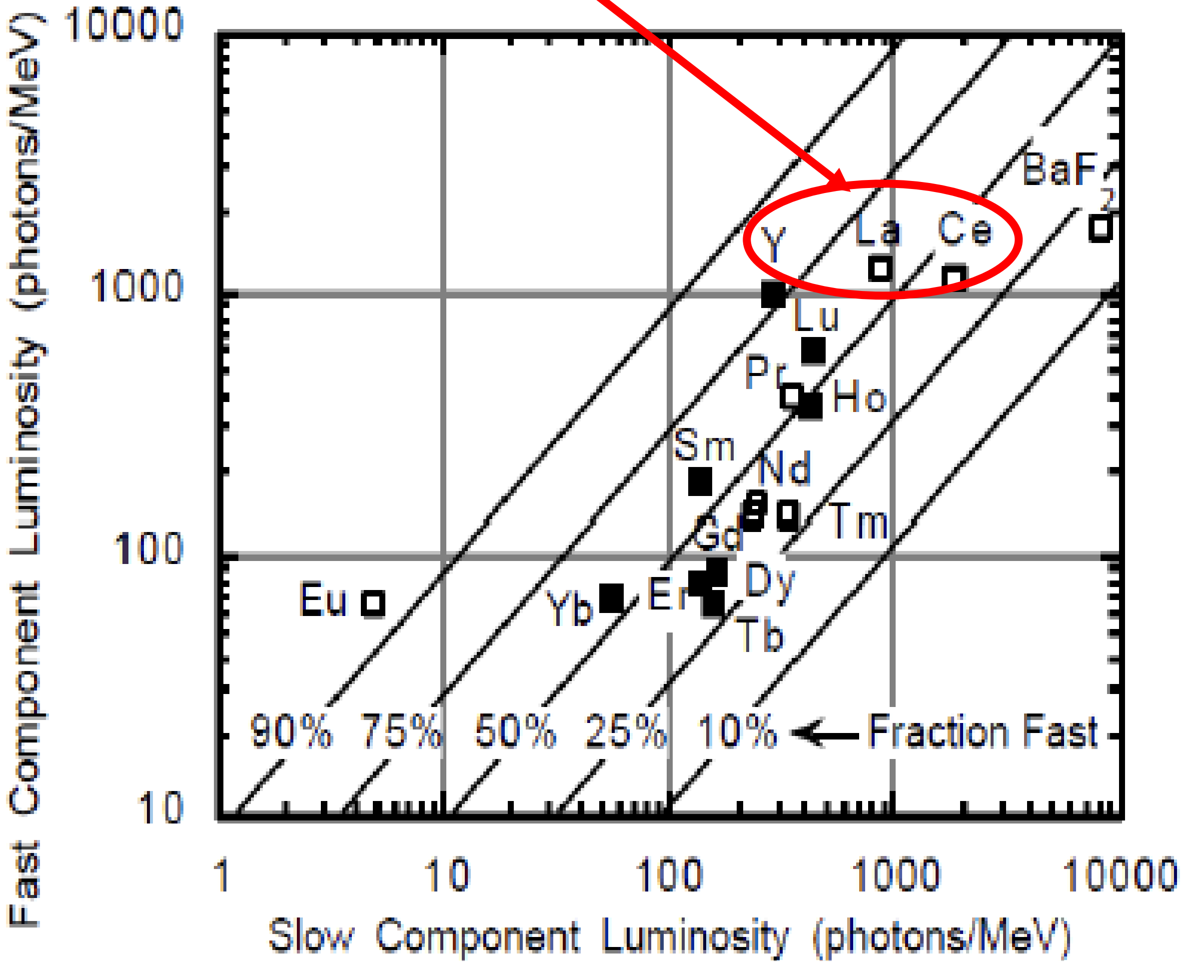

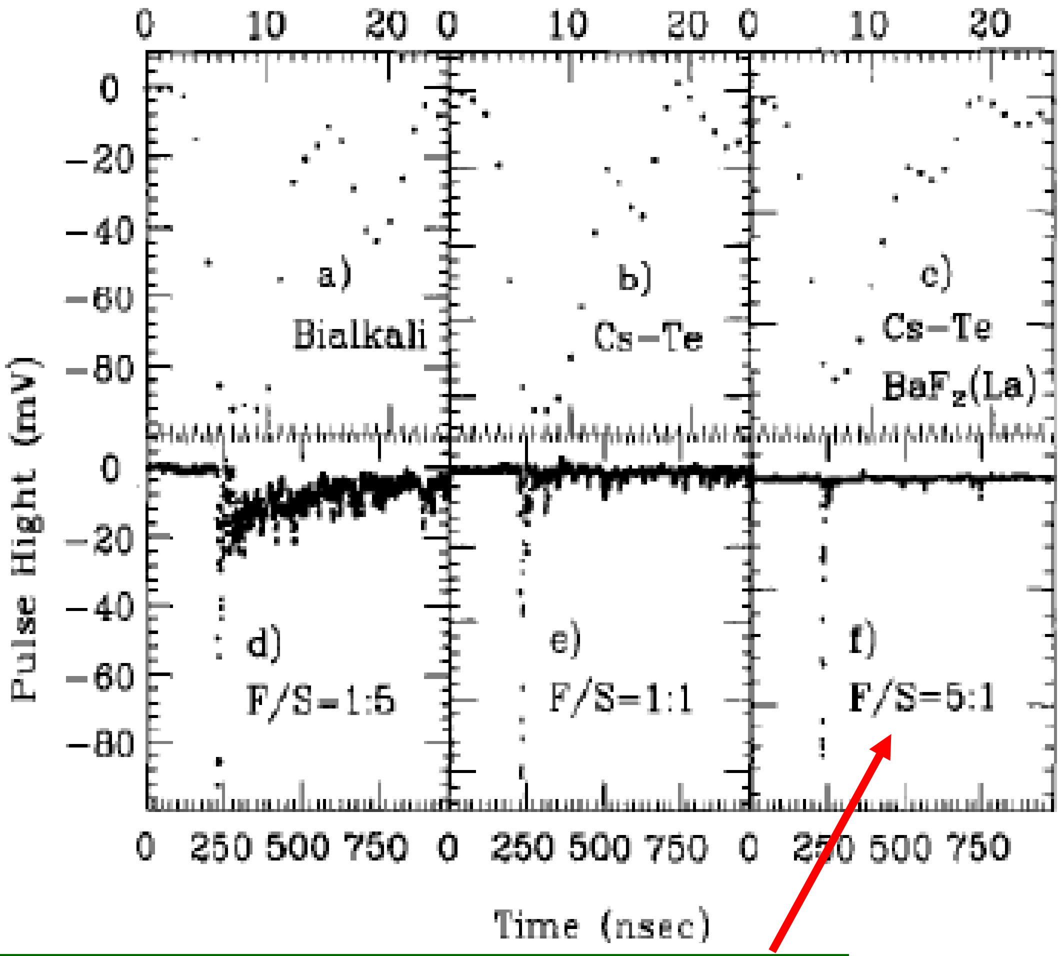

Cs-Te cathode plus La doping raises F/S from 1/5 to 5/1, NIMB **91** (1991) 61-66

Transmittance of BaF_2:La and BaF_2:La/Ce

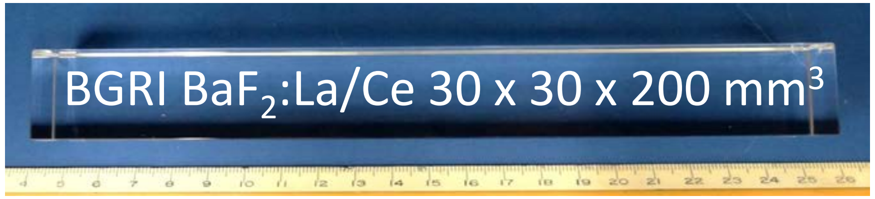

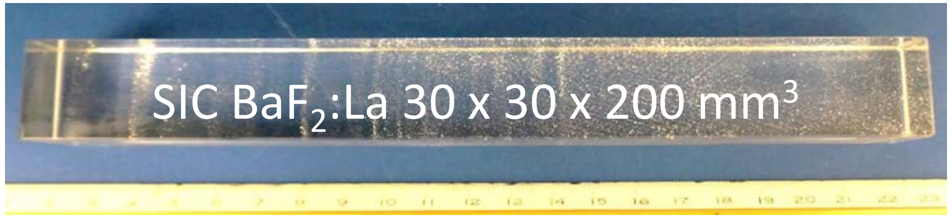

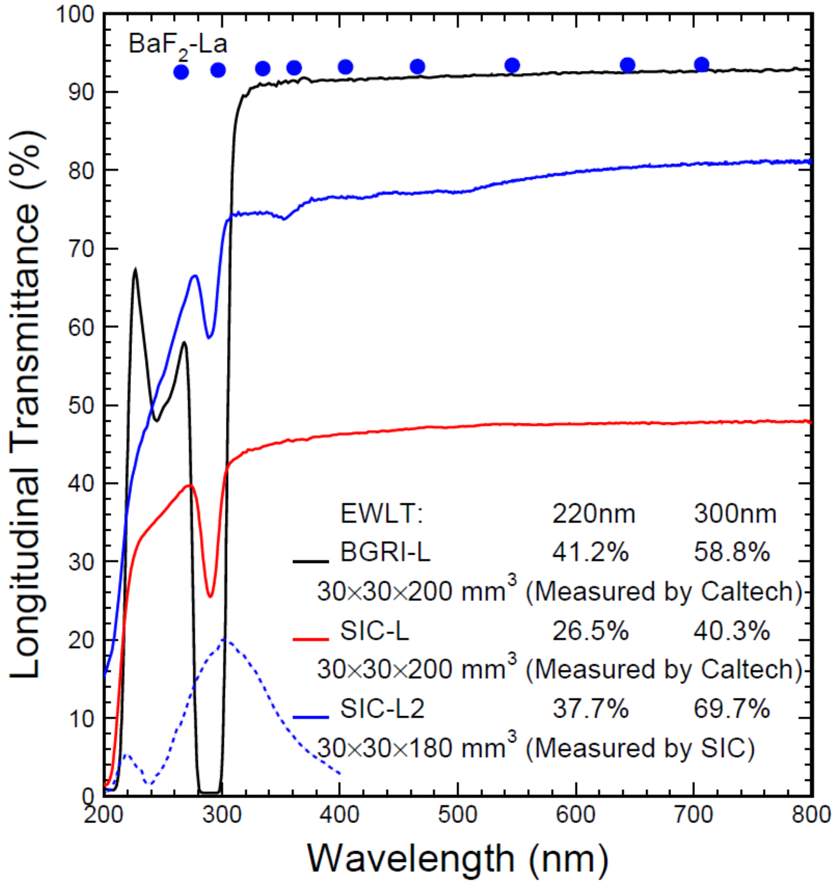

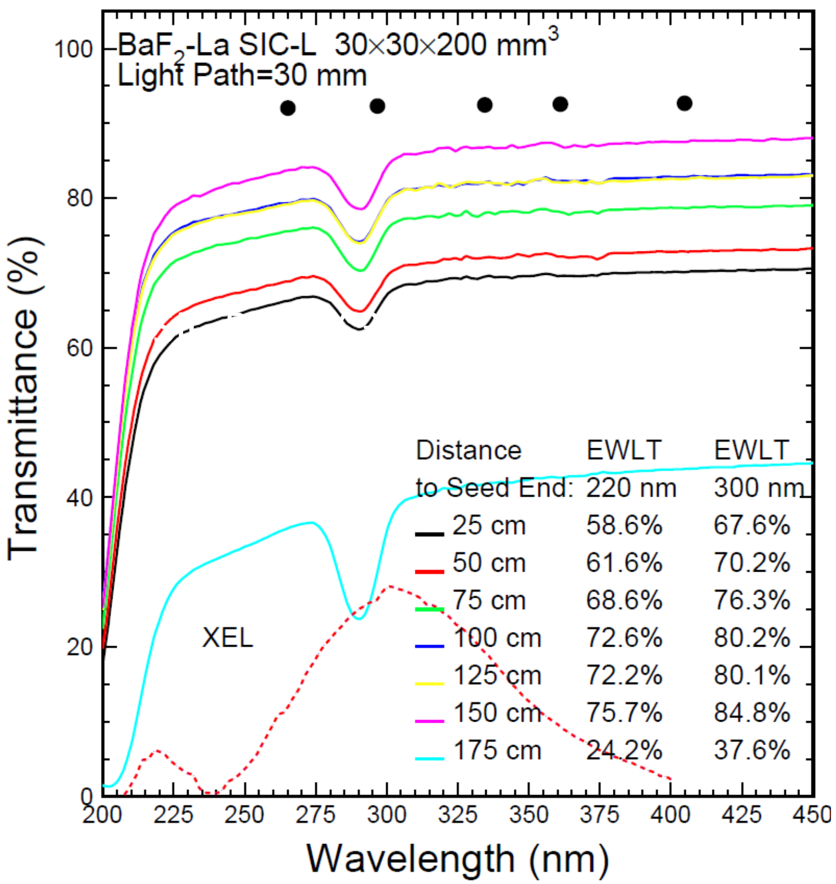

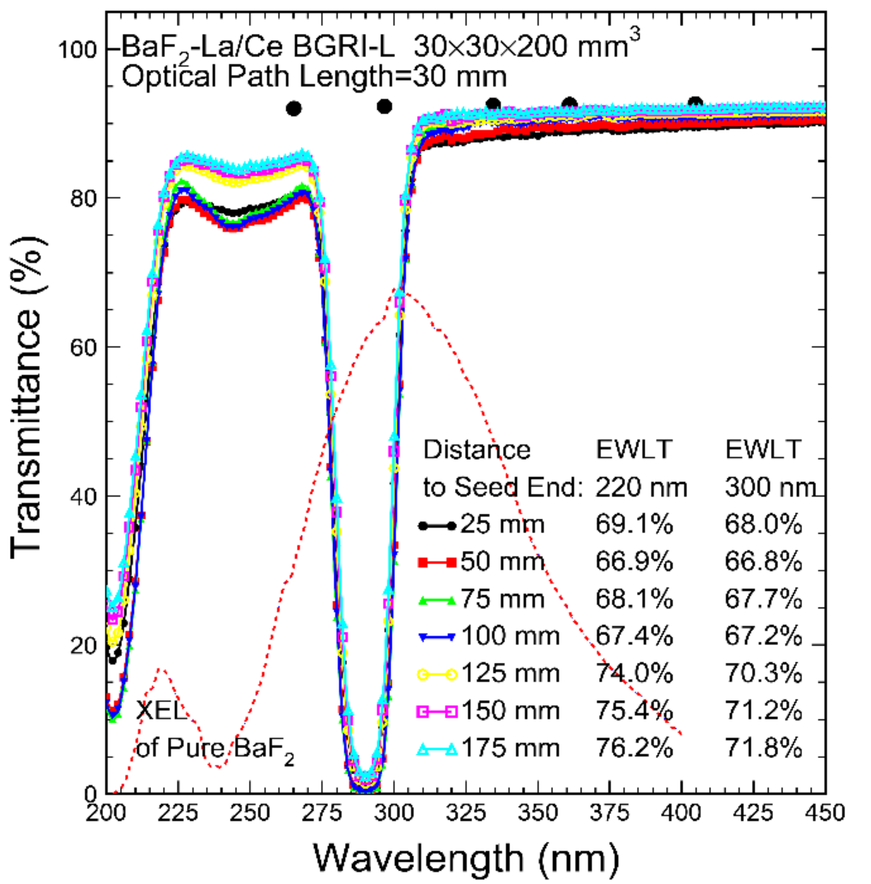

Absorptions observed in La and La/Ce doped BaF_2:IEEE TNS **66** (2019) 506-518

Yttrium Doped Small BaF_2 Samples

Increased F/S ratio observed in BGRI BaF_2:Y crystals: Proc. SPIE 10392 (2017)

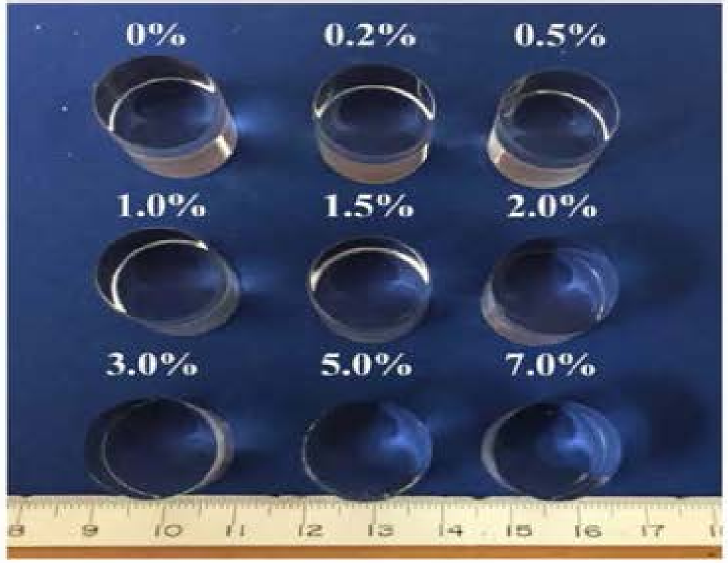

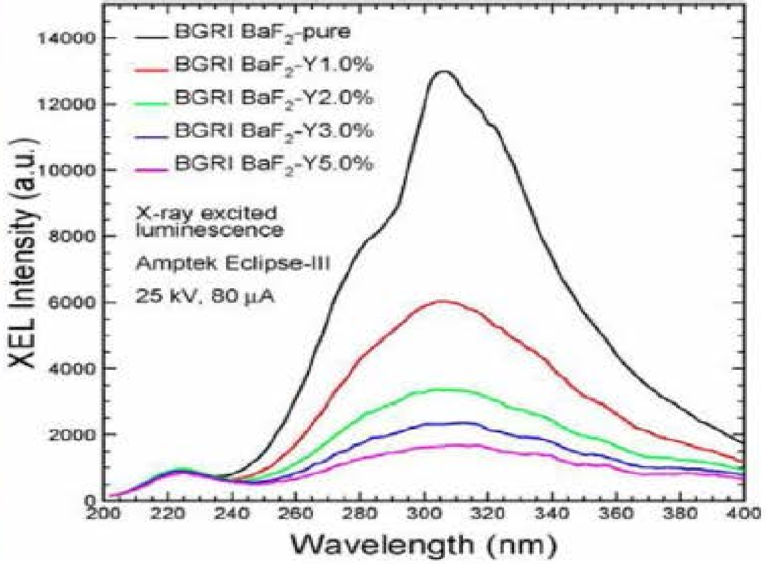

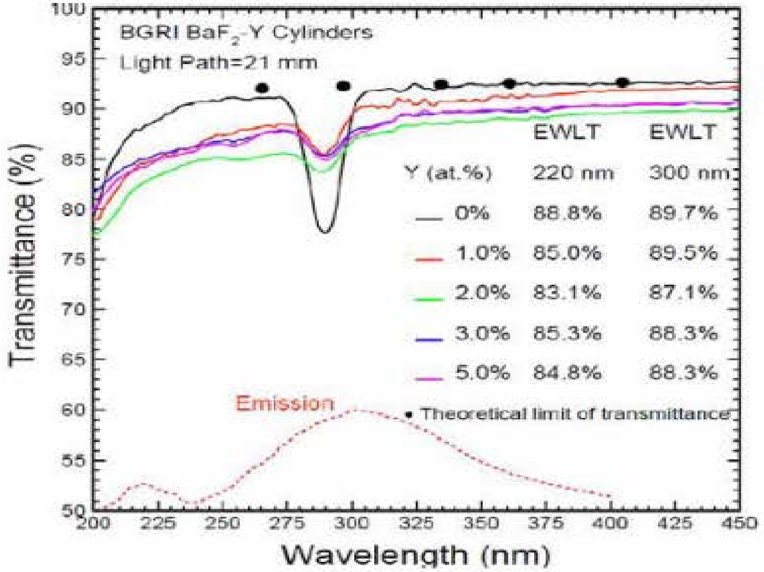

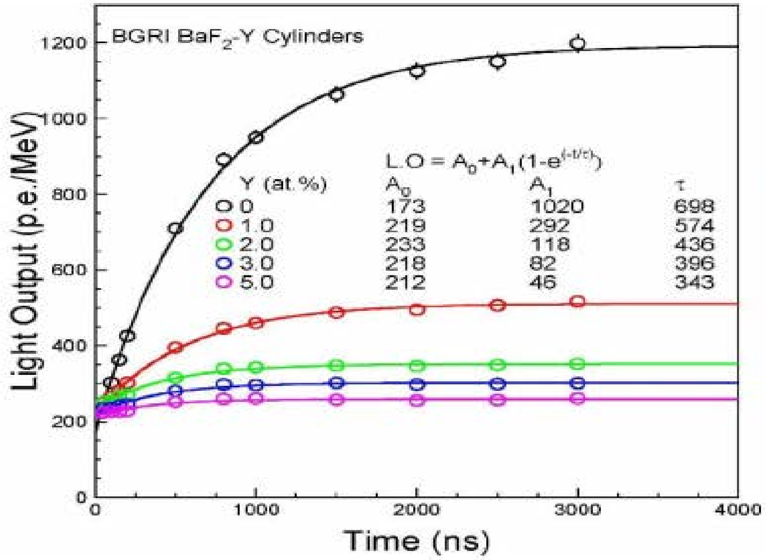

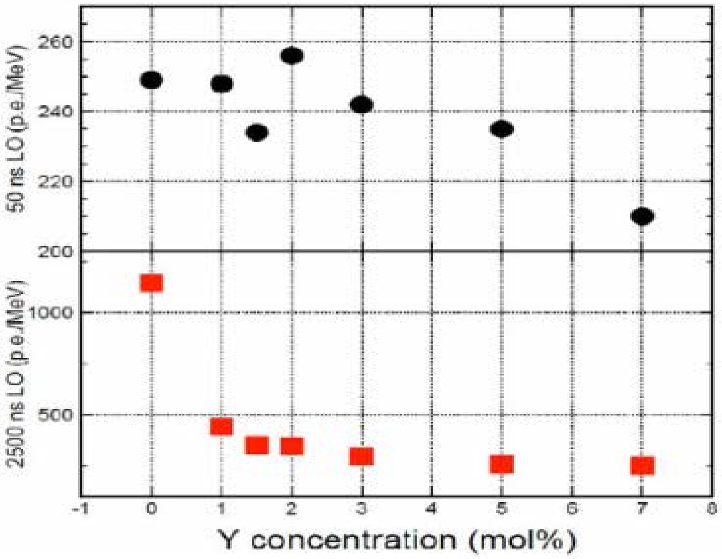

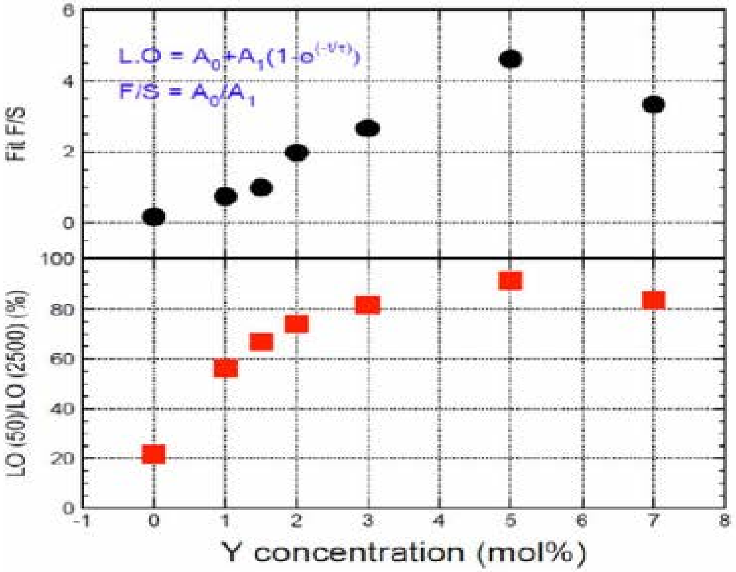

APS Beam Test: BaF_2:Y, BaF_2, ZnO:Ga & LYSO

X-ray bunches with 2.83 ns spacing in septuplet are clearly resolved by ultrafast BaF_2:Y and BaF_2 crystals: NIMA 240 (2019) 223-239

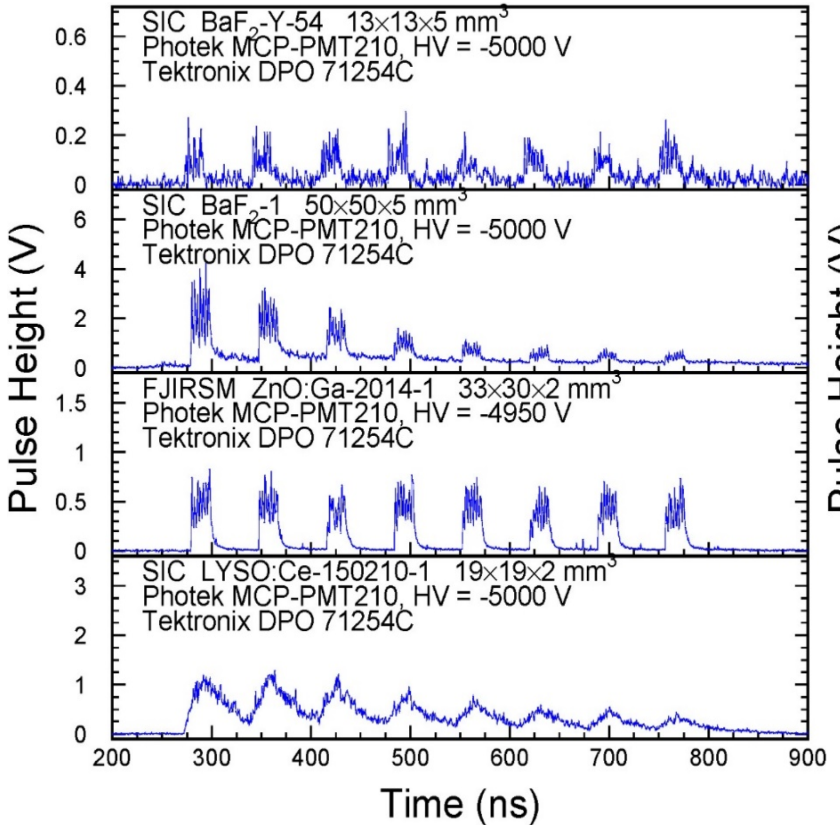

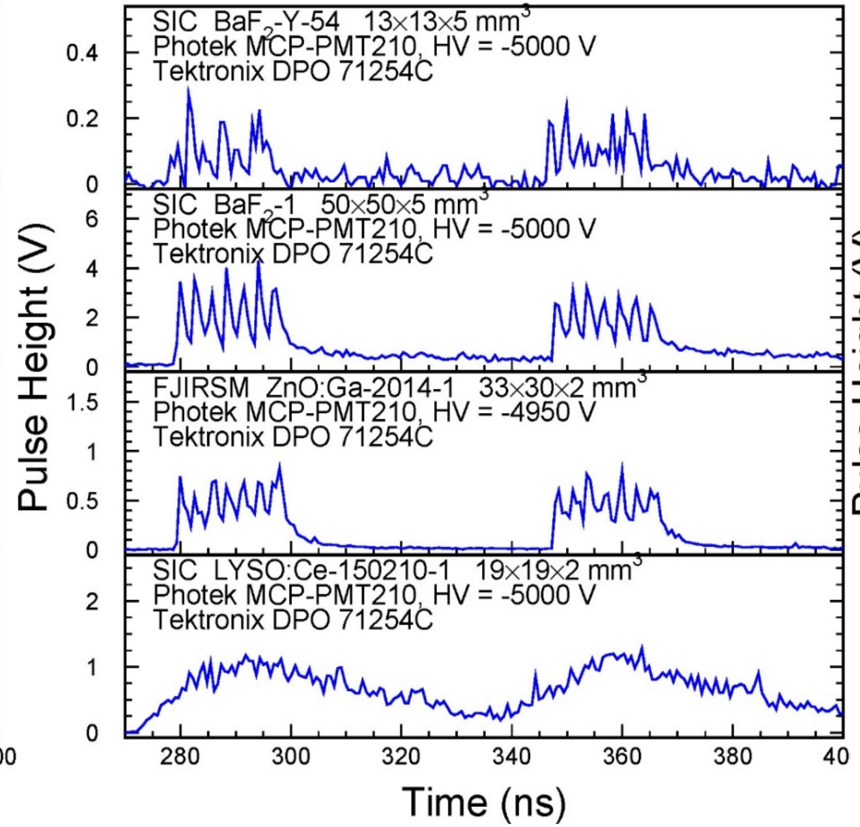

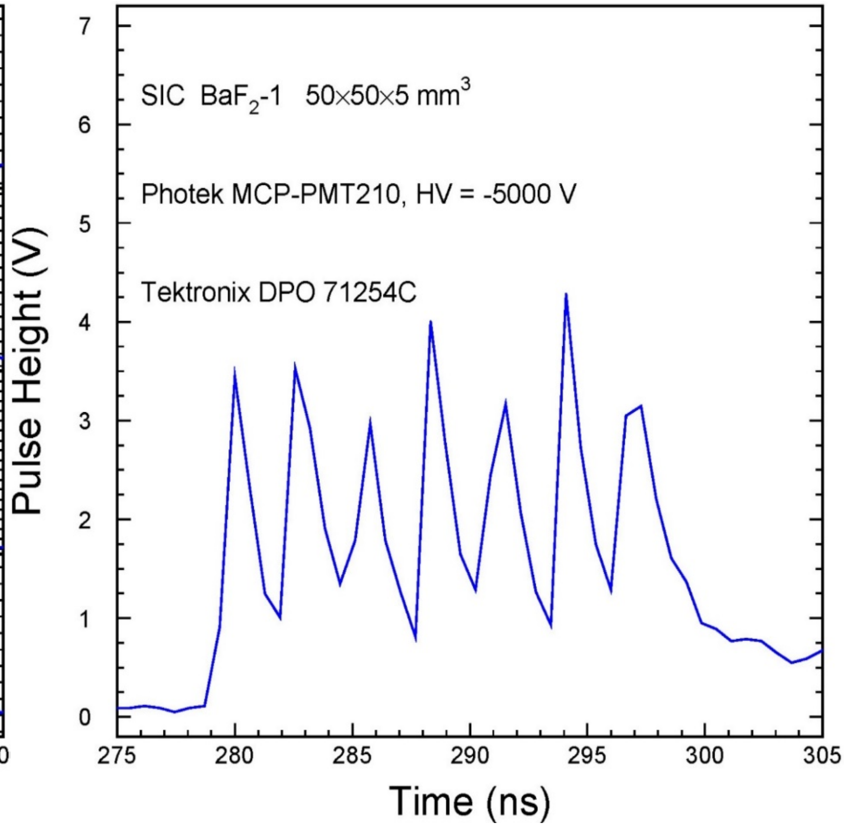

Amplitude reduction in BaF_2 and LYSO due to space charge in PMT from slow scintillation, but not in BaF_2:Y

SIC BaF_2:Y-2017

F: 150 p.e./MeV, F/S: 1.5
F/T LRU: 10%/6%, δ_F:-1.2%/X_0

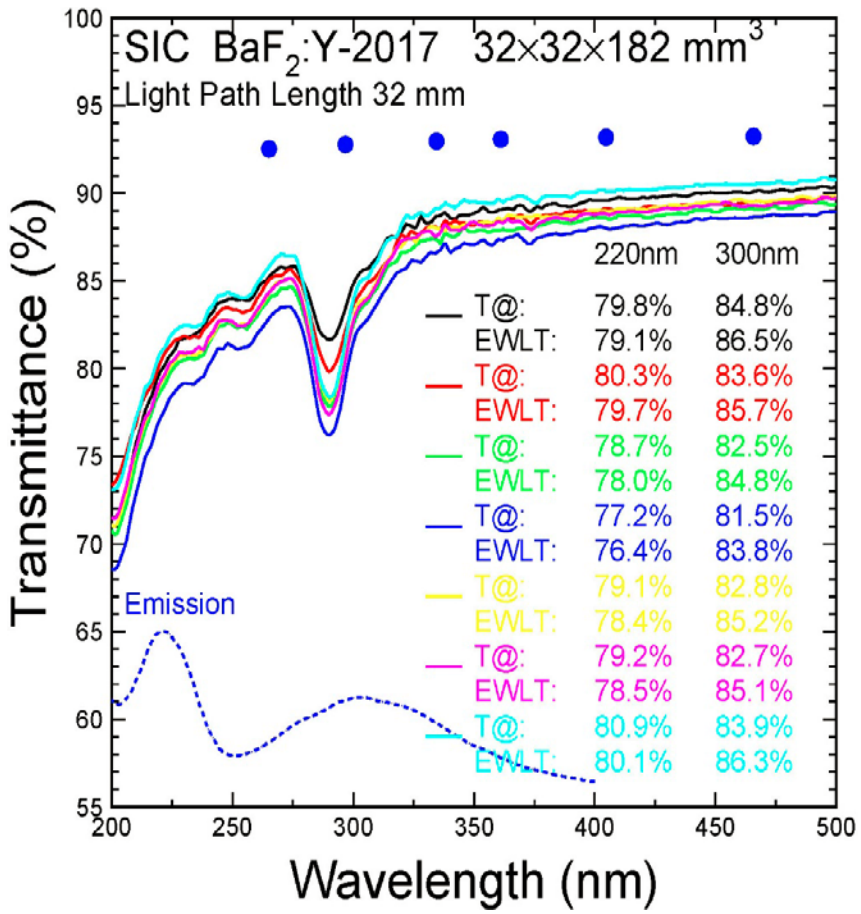

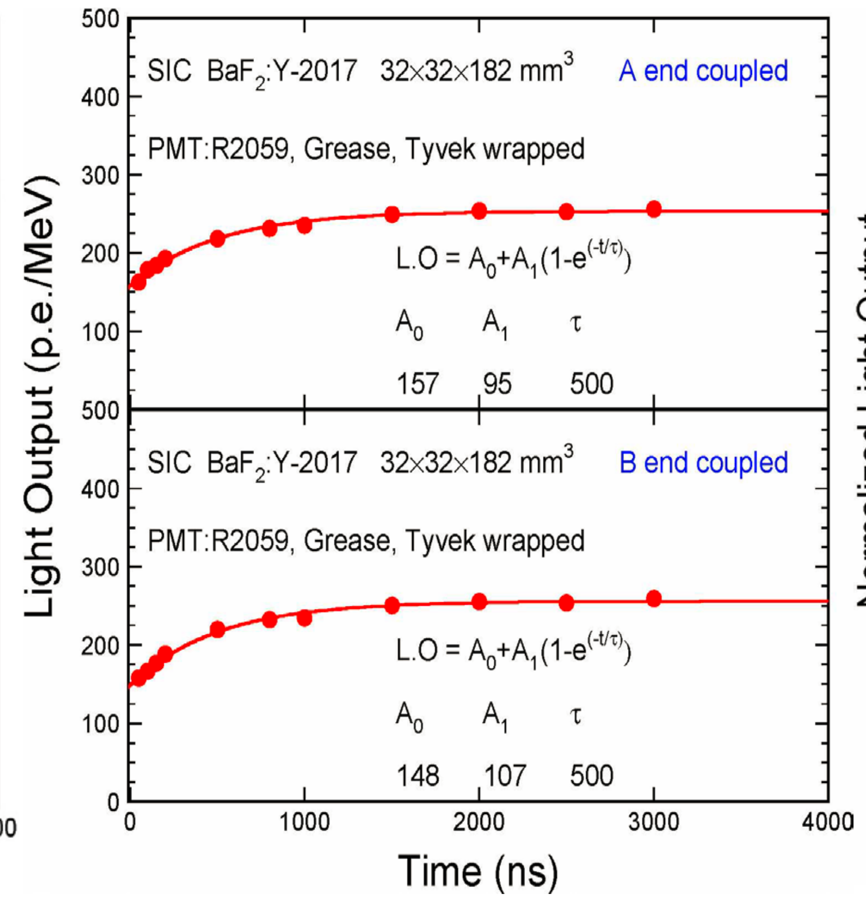

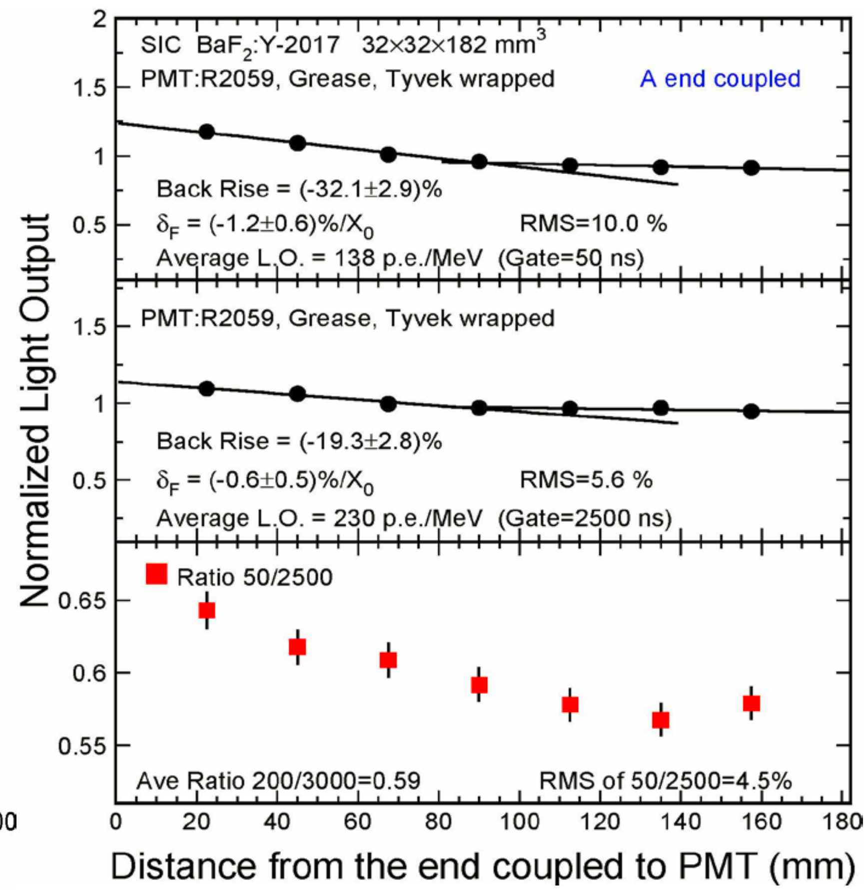

SIC BaF_2:Y-2019

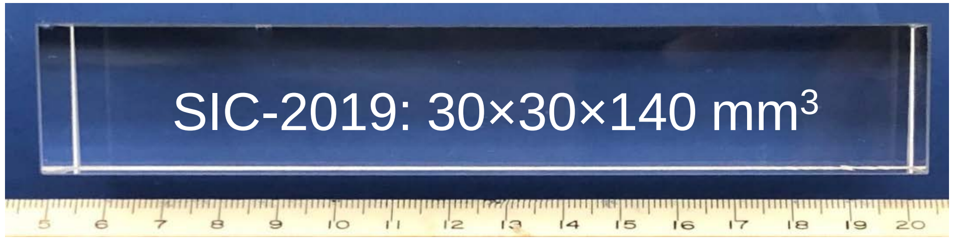

F: 130 p.e./MeV, F/S: 2

F/T LRU: 13%/6% %, δ_F:-3.3%/X_0

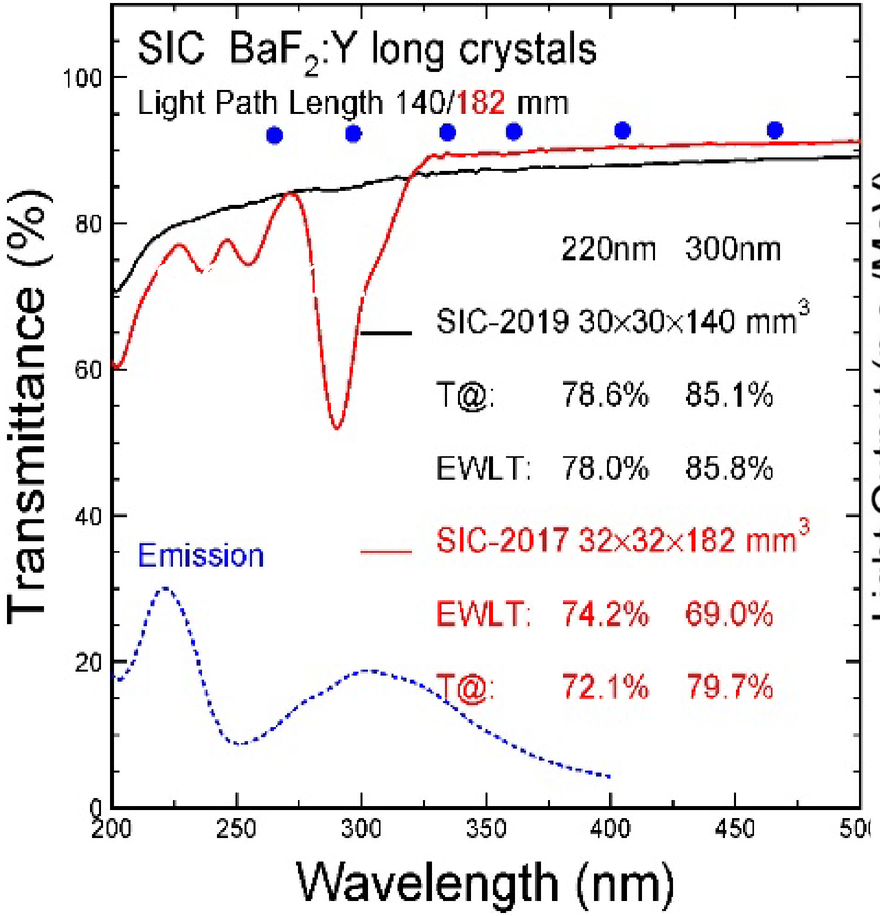

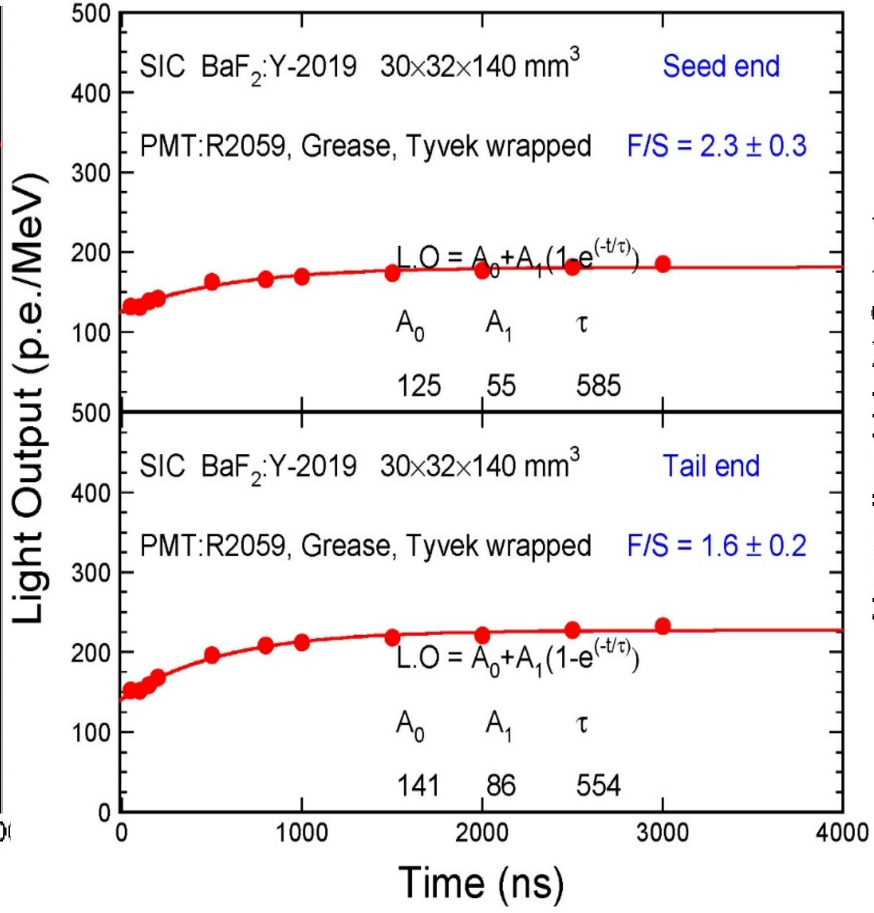

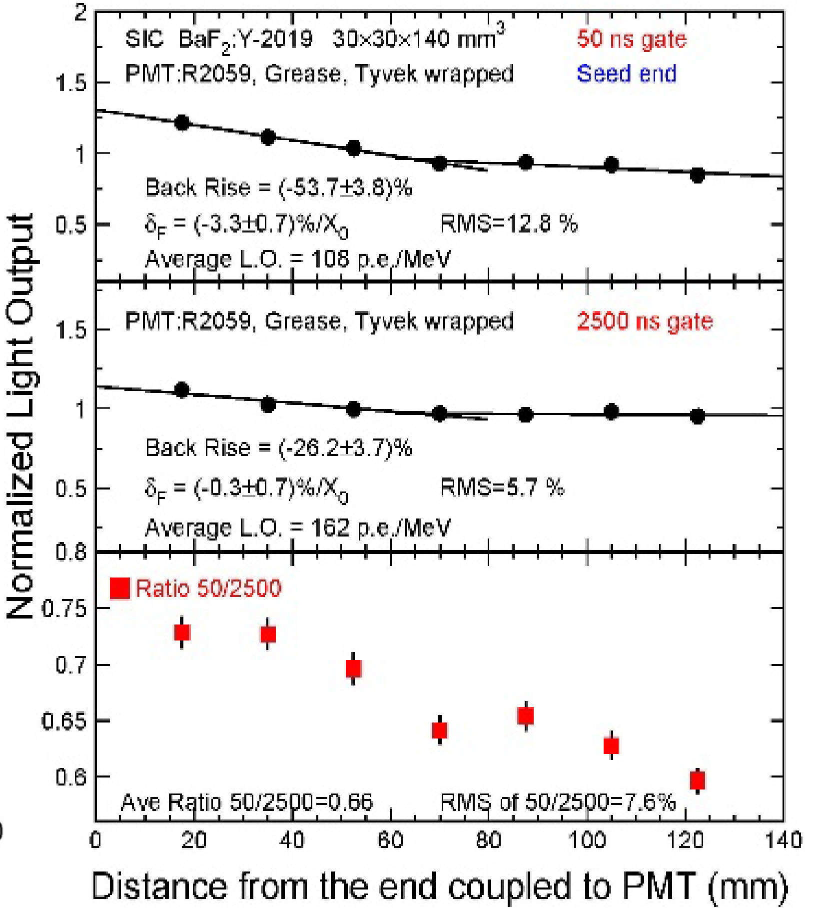

SIC BaF_2:Y-2020

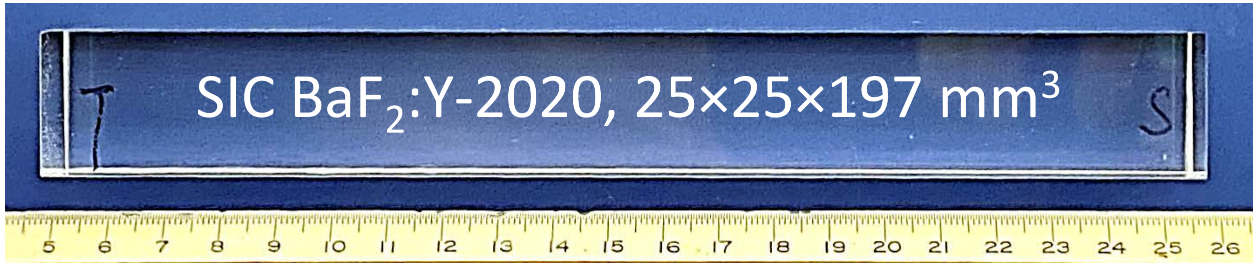

F: 100 p.e./MeV, F/S: 2
F/T LRU: 10%/5% %, δ_F:-0.3%/X_0

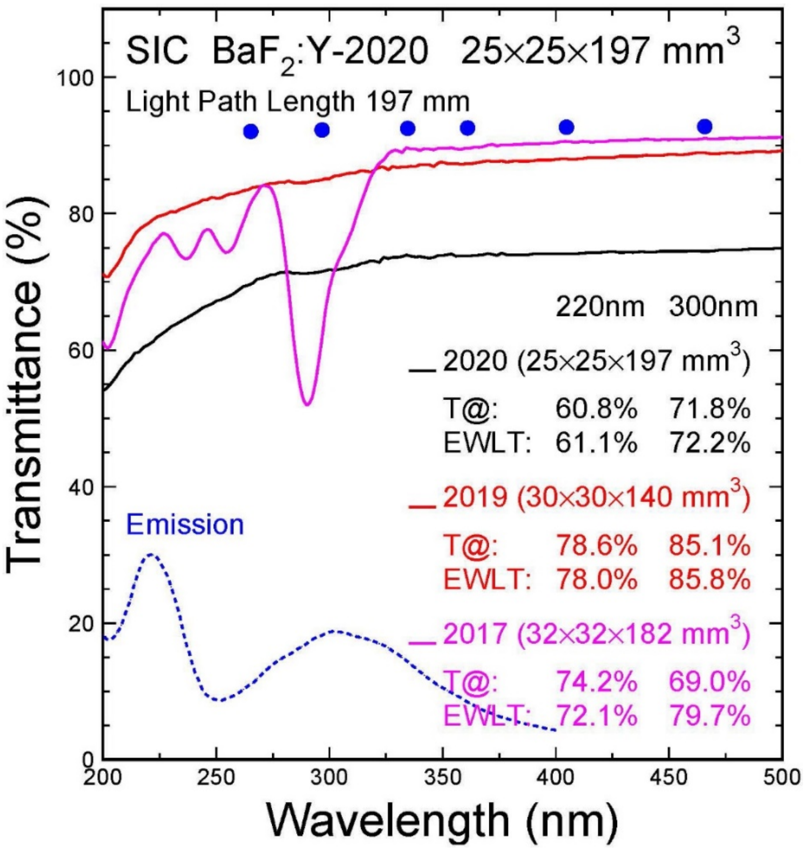

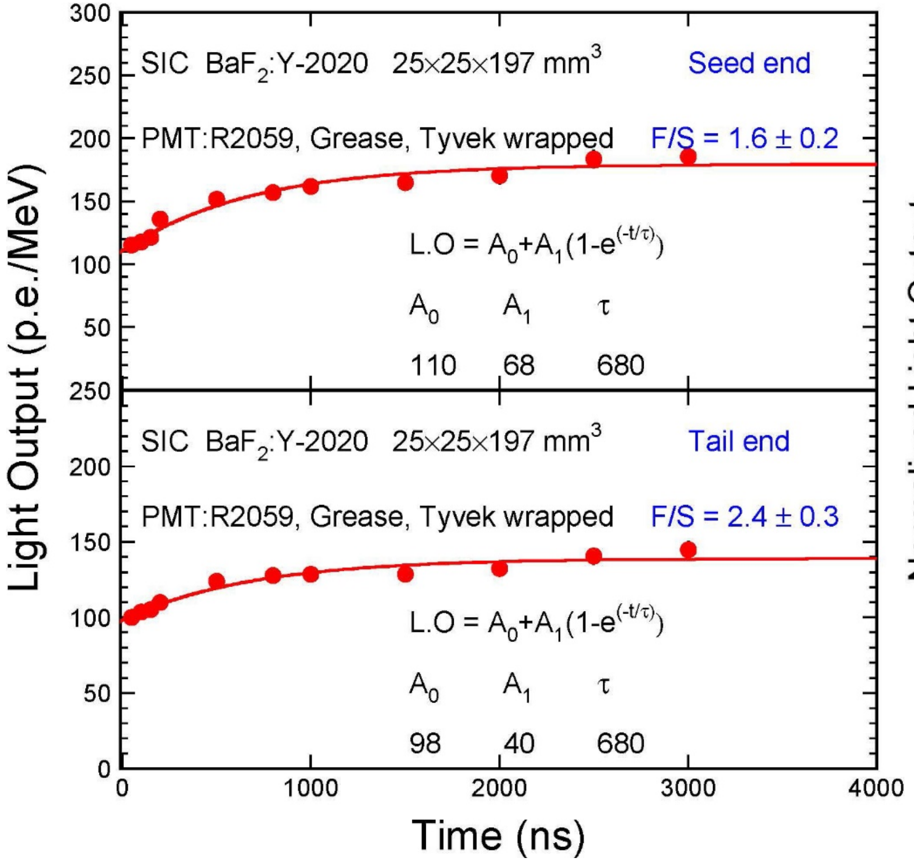

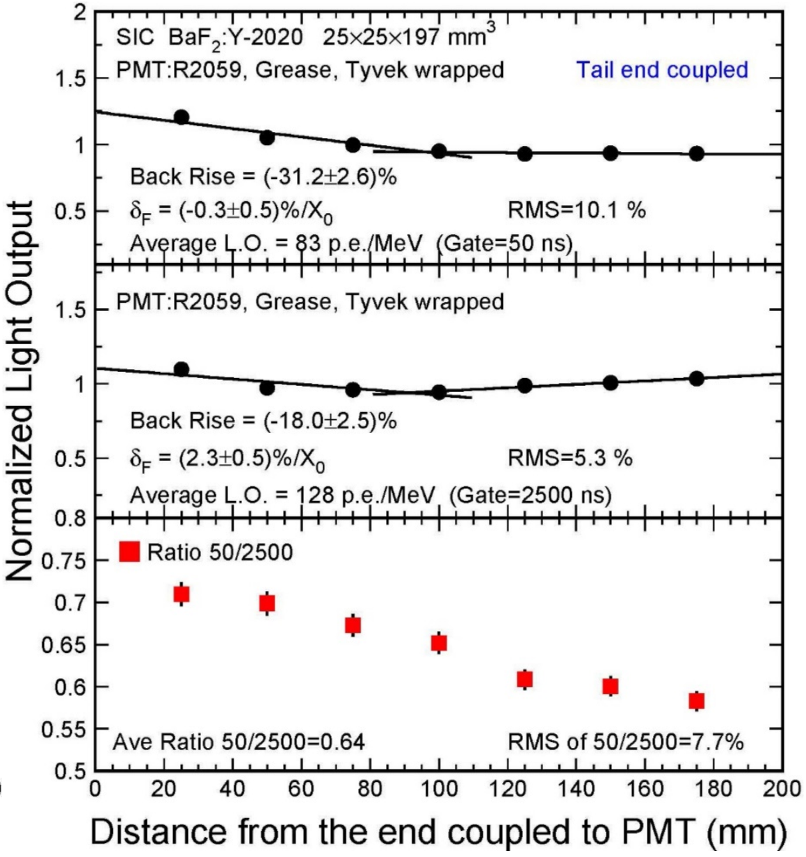

SIC BaF_2:Y-2020: Transverse T

A variation of slow emission intensity and more scattering centers starting from 15 cm from the seed

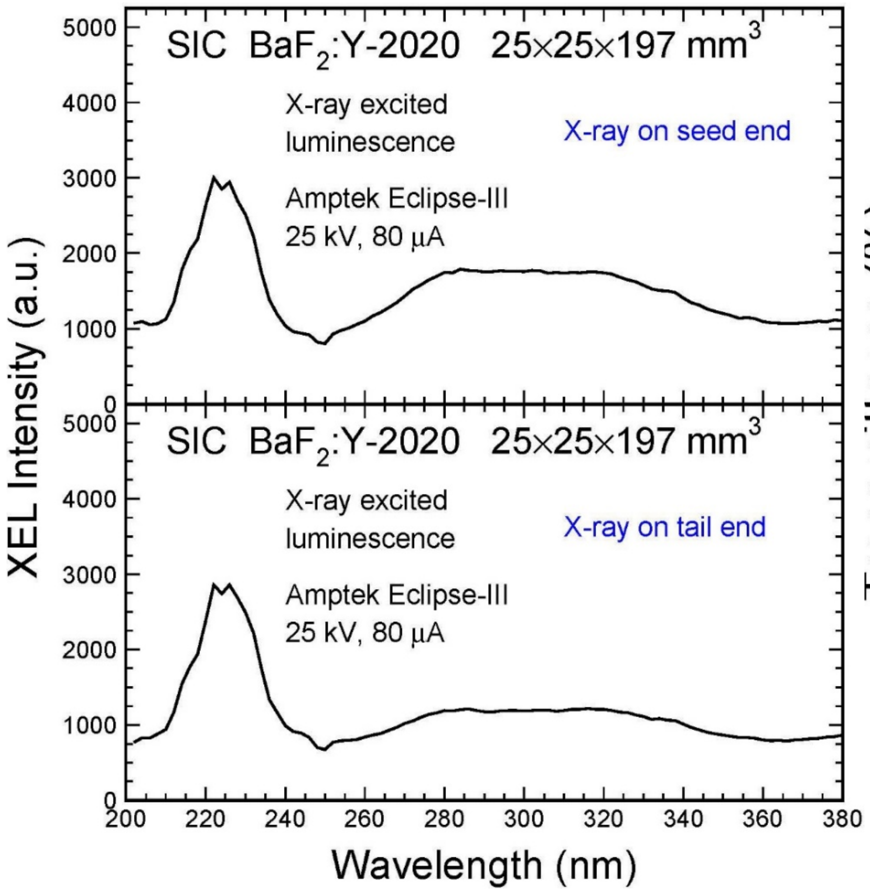

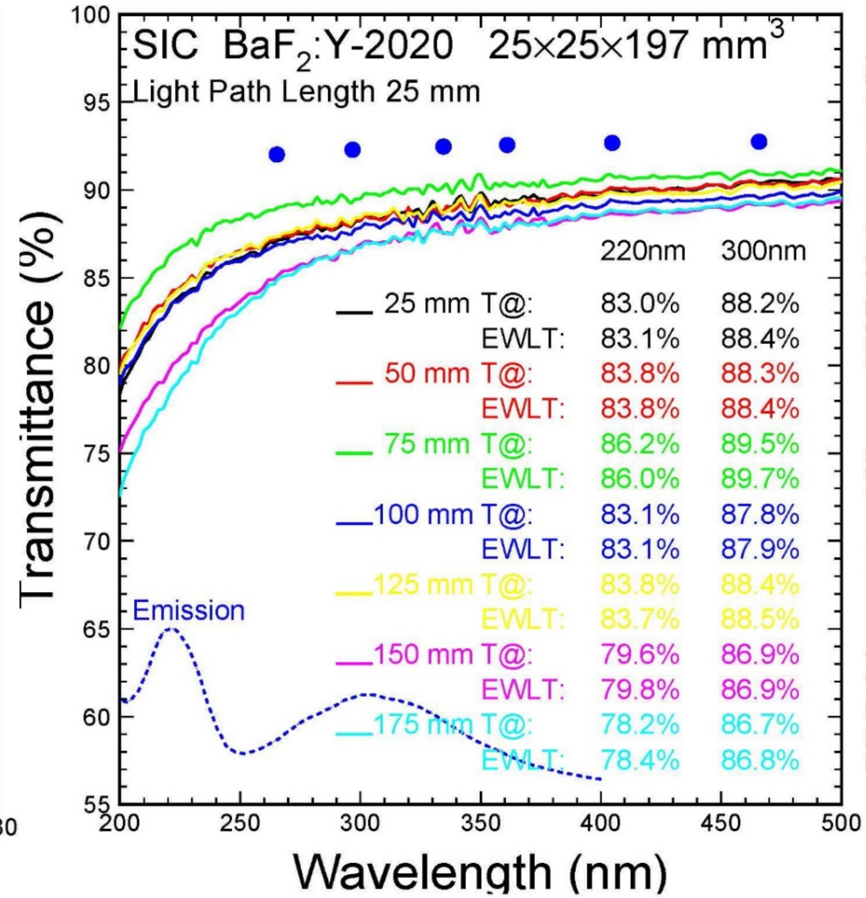

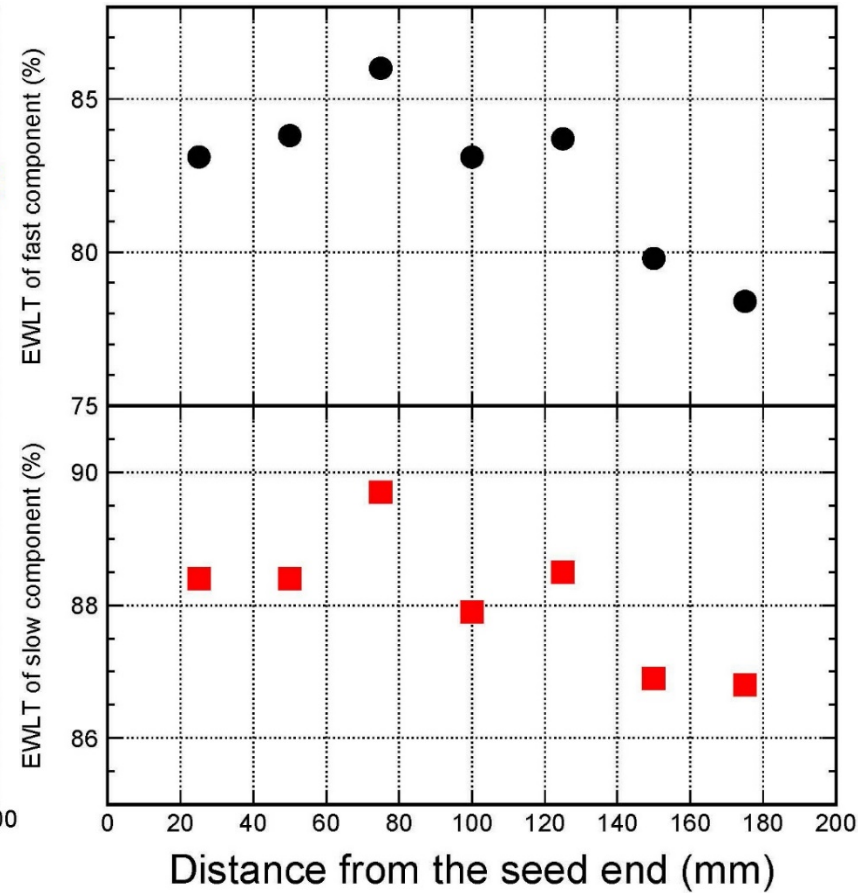

Summary: SIC BaF_2:Y Long Crystals

ID	Dimension (mm^3)	EWLT Fast (%)	EWLT Slow (%)	Coupling end	Basic Scintillation Performance ^{22}Na/α source @ 1/8 length from the coupling end					Light Response Uniformity		
					50 ns LO (p.e./MeV)	2500 ns LO (p.e./MeV)	LO(50) /LO(2500)	F	F/S	50 ns LO	2500 ns LO	LO(50)/ LO(2500)
SIC BaF_2:Y-2017	32×32×182	72.1	79.7	A	162	253	0.64	157	1.7	138 (10.0%)	230 (5.6%)	0.59 (4.5%)
				B	158	254	0.62	148	1.4	116 (19.1%)	200 (16.4%)	0.57 (3.7%)
SIC BaF_2:Y-2019	30×30×140	78.0	85.8	A	132	181	0.73	125	2.3	108 (12.8%)	162 (5.7%)	0.66 (7.6%)
				B	152	227	0.67	141	1.6	117 (15.6%)	177 (14.9%)	0.66 (1.5%)
SIC BaF_2:Y-2020	25×25×197	61.1	72.2	Seed	115	183	0.63	110	1.6	88 (17.7%)	136 (20.5%)	0.64 (2.8%)
				Tail	100	141	0.71	98	2.4	83 (10.1%)	128 (5.3%)	0.64 (7.7%)

BGRI BaF_2:Y-2017

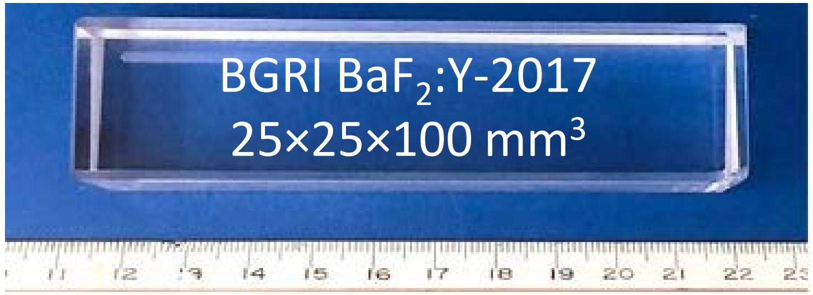

F: 150 p.e./MeV, F/S: 1.5
F/T LRU: 12%/7% %, δ_F:-4.2%/X_0

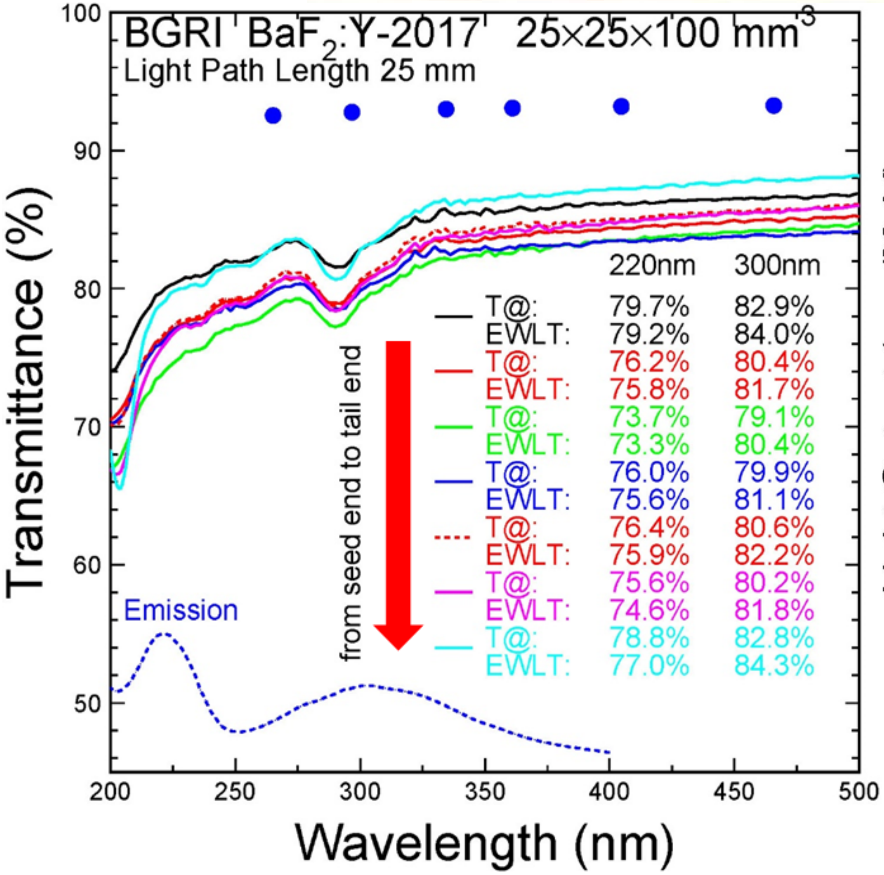

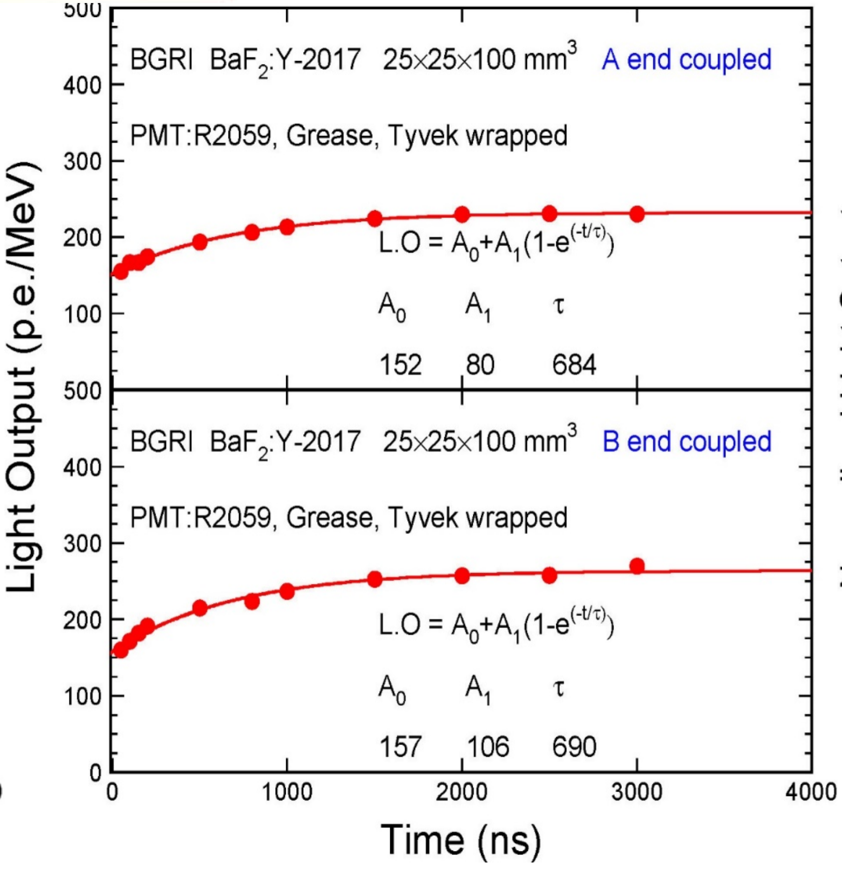

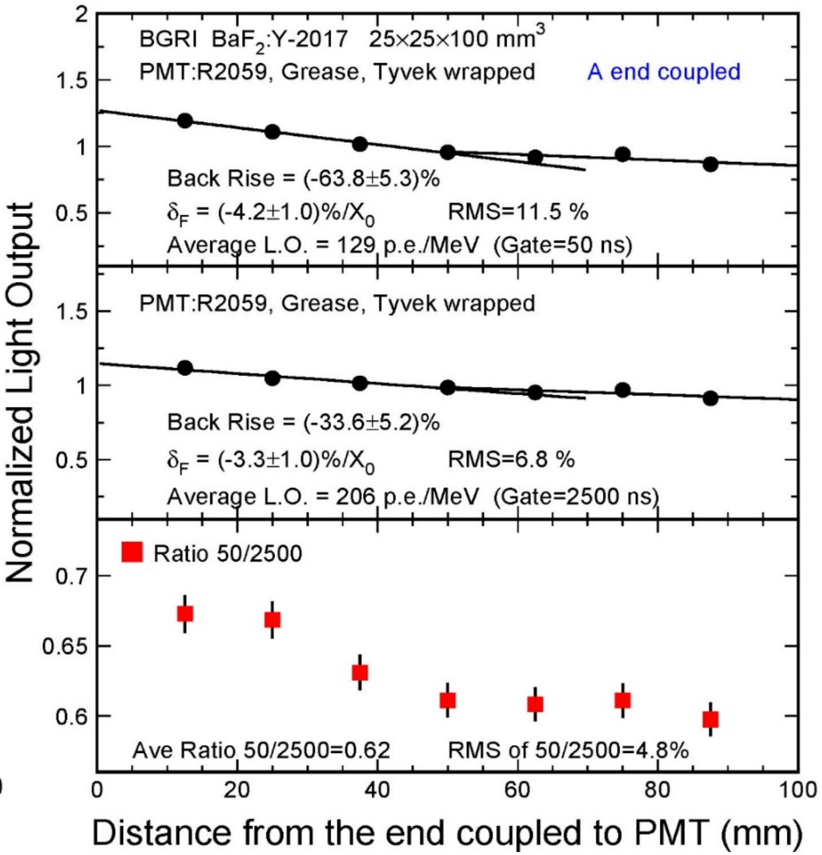

BGRI BaF_2:Y-2020

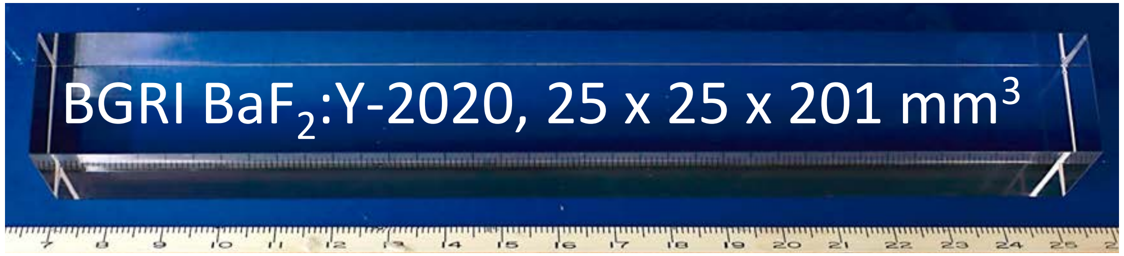

F: 125 p.e./MeV, F/S: 0.9
F/T LRU: 15%/9% %, δ_F:-2.1%/X_0

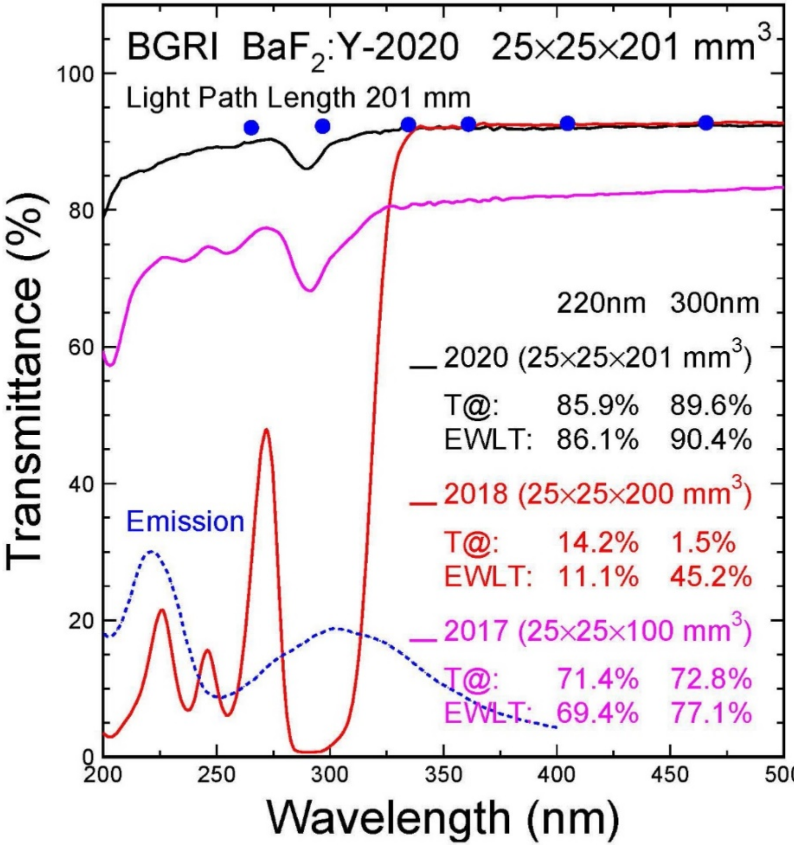

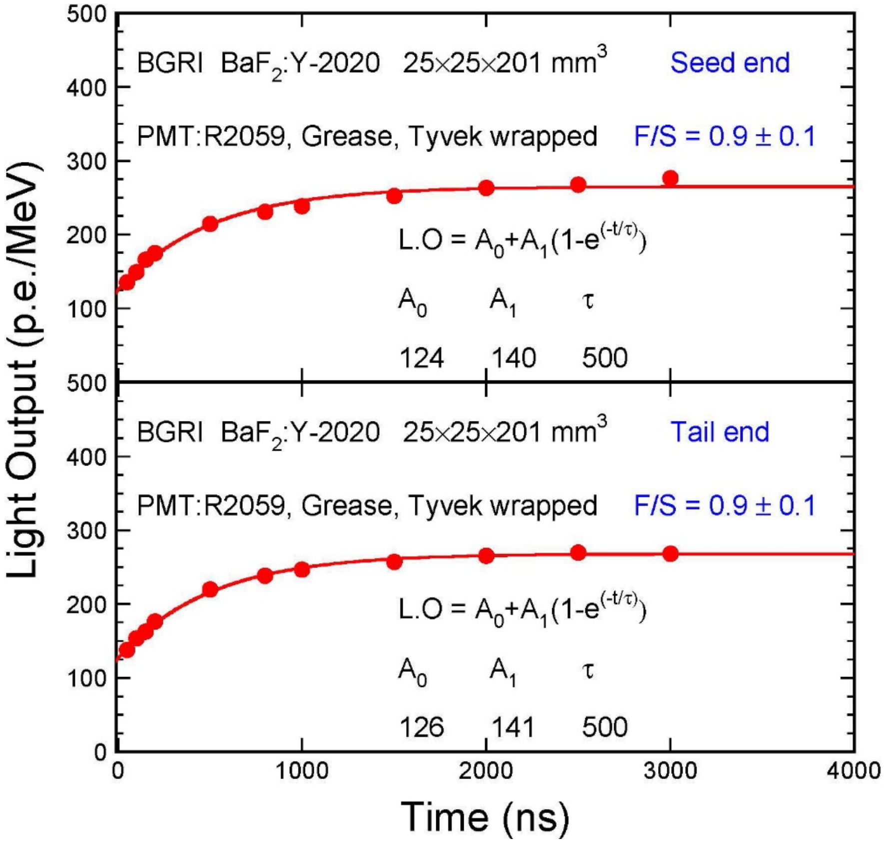

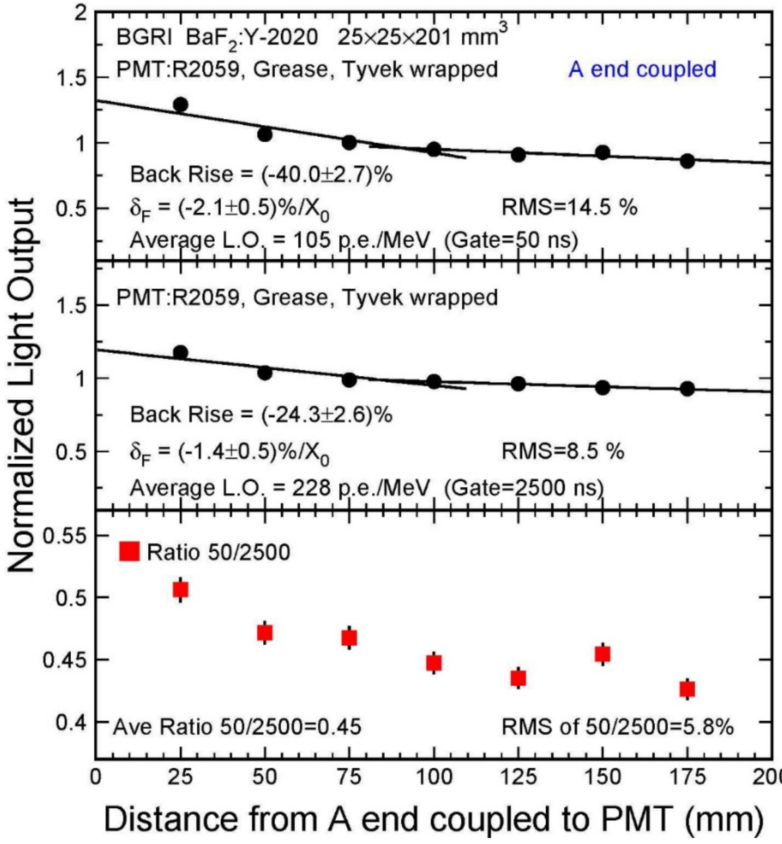

BGRI BaF_2:Y-2020: Transverse T

A variation of slow emission intensity and good optical quality along the crystal length

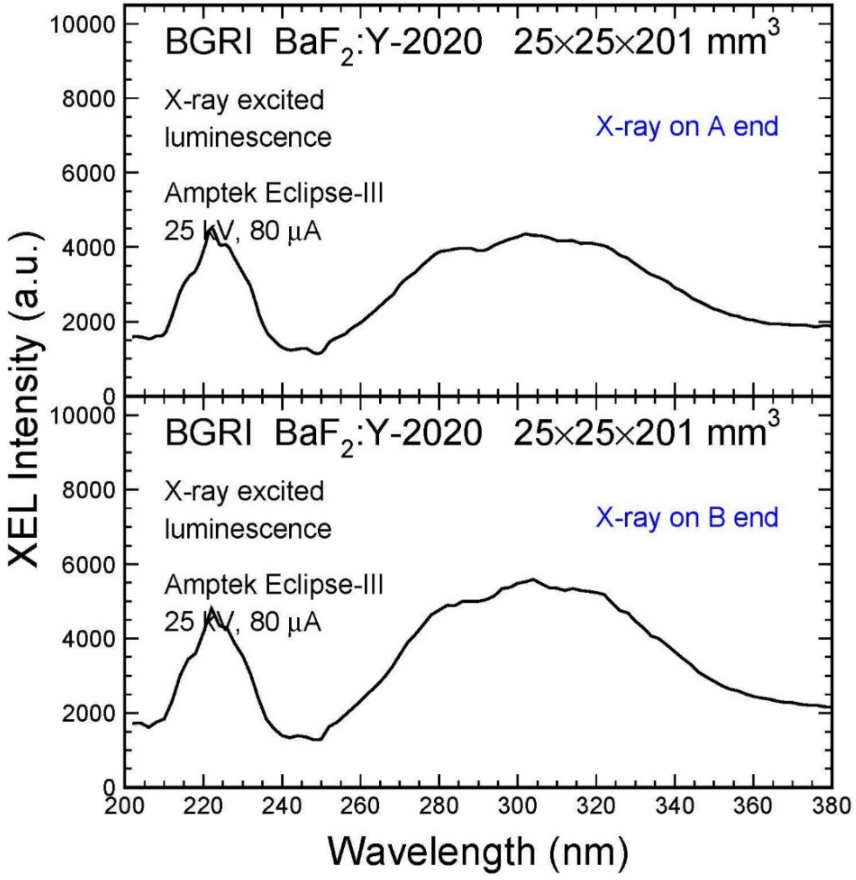

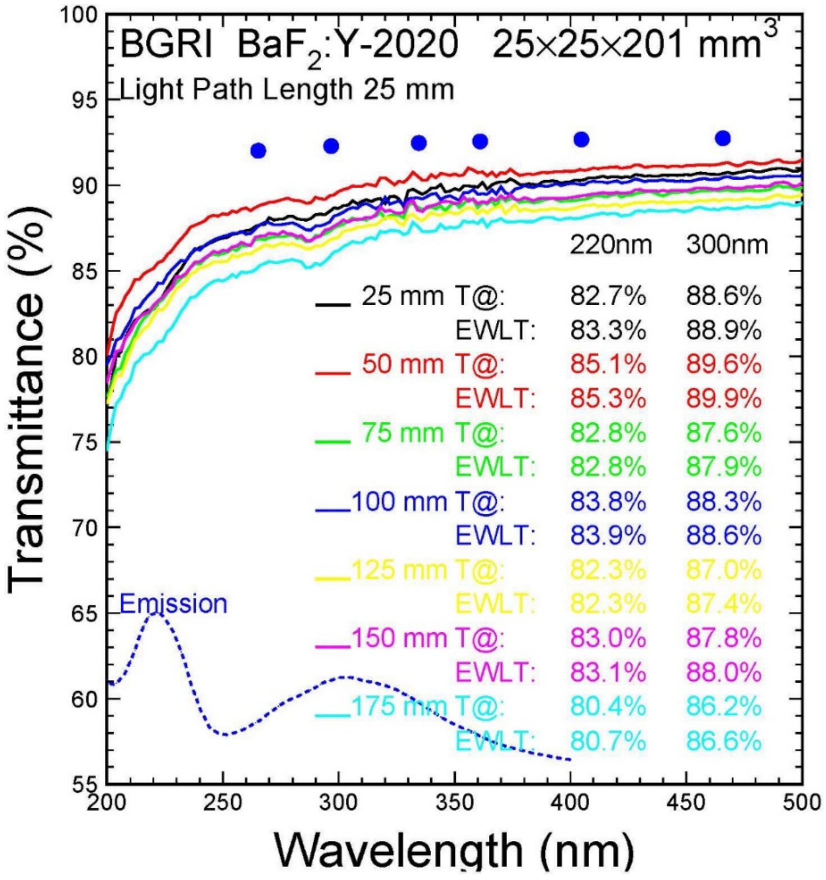

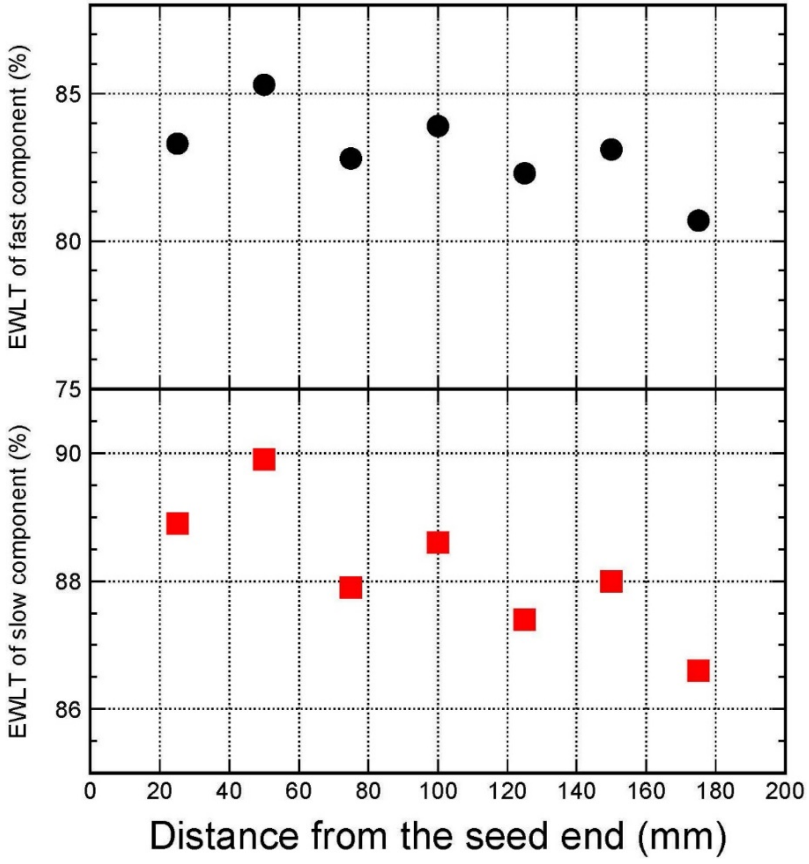

Summary: BGRI BaF_2:Y Long Crystals

ID	Dimension (mm^3)	EWLT Fast (%)	EWLT Slow (%)	Coupling end	Basic Scintillation Performance Source @ 1/8 length from the coupling end					Light Response Uniformity		
					50 ns LO (p.e./MeV)	2500 ns LO (p.e./MeV)	LO(50) /LO(2500)	F	F/S	50 ns LO	2500 ns LO	LO(50)/ LO(2500)
BGRI BaF_2:Y-2017	25×25×100	69.4	77.1	A	155	231	0.67	152	1.9	129 (11.5%)	206 (6.8%)	0.62 (4.8%)
				B	160	258	0.62	157	1.5	129 (15.4%)	214 (13.7%)	0.60 (2.1%)
BGRI BaF_2:Y-2018	25×25×200	11.1	45.2	A	133	317	0.42	203*	NA	83 (30.6%)	229 (20.4%)	0.35 (9.4%)
				B	133	265	0.52	159*	NA	89 (26.4%)	228 (8.7%)	0.38 (17.2%)
BGRI BaF_2:Y-2020	25×25×201	61.1	72.2	A	135	268	0.50	124	0.9	105 (14.5%)	228 (8.5%)	0.45 (5.8%)
				B	138	270	0.51	126	0.9	106 (17.1%)	221 (14.7%)	0.47 (3.1%)

*Only one component with 30~50 ns decay time is observed, but no ultrafast component

γ-Ray Induced Damage in BaF_2

BaF_2 shows saturated damage from 10 krad to 100 Mrad, indicating good radiation resistance against γ-rays
IEEE TNS **63** (2016) 612-619

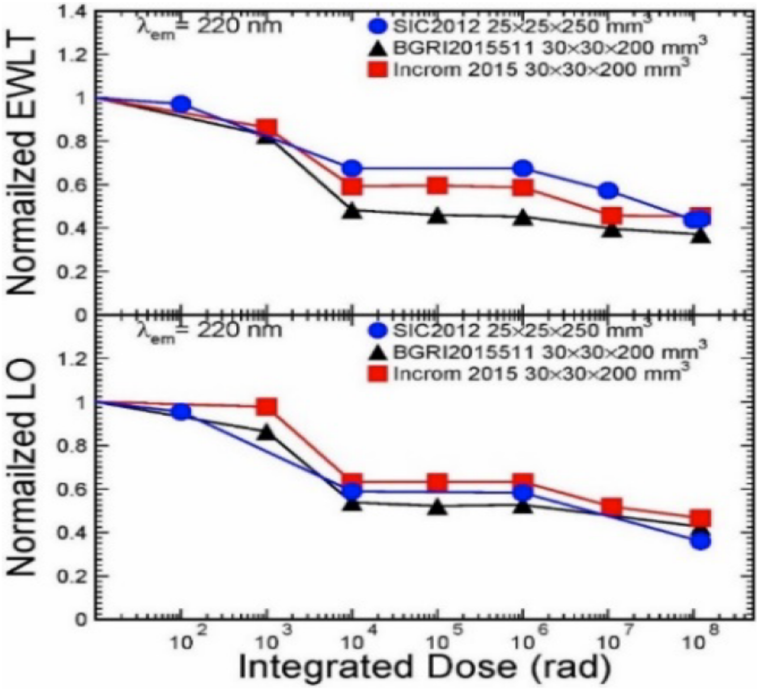

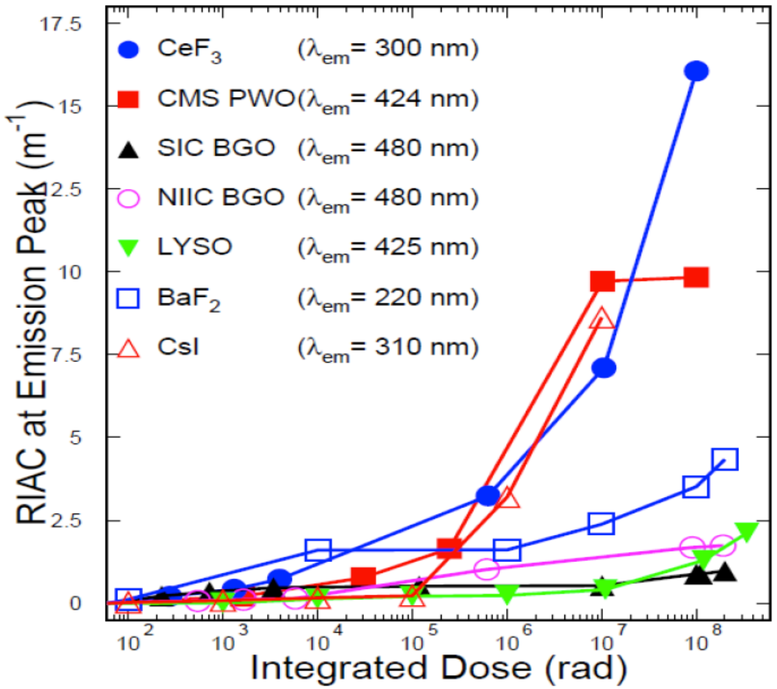

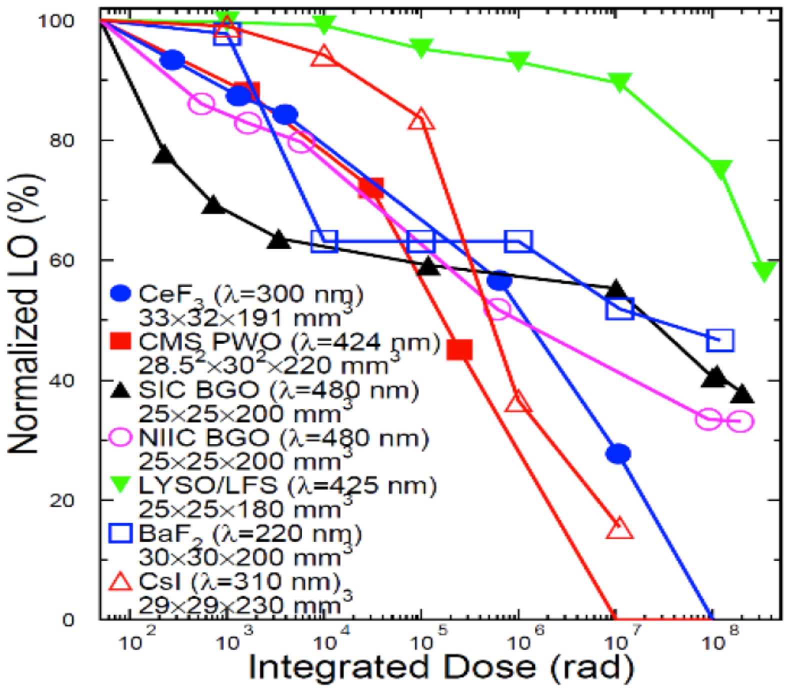

Hadron Induced Damage in BaF_2

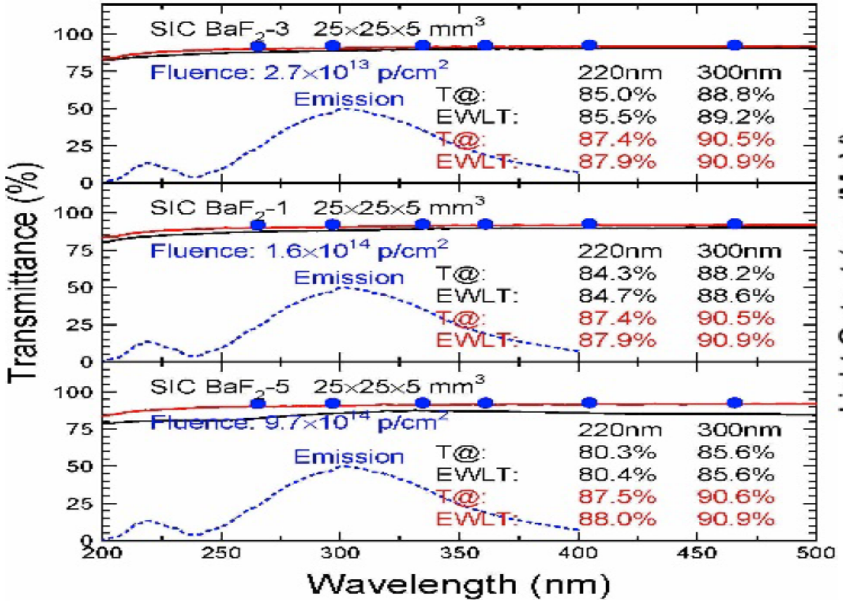

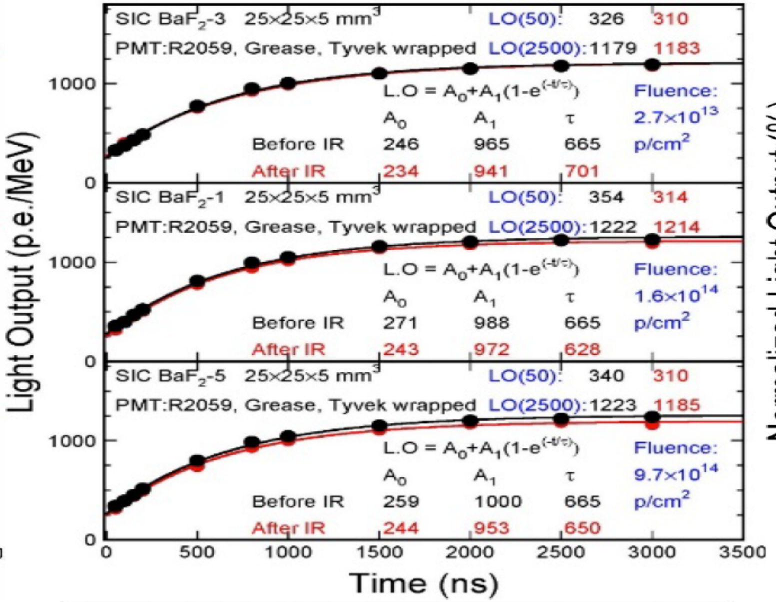

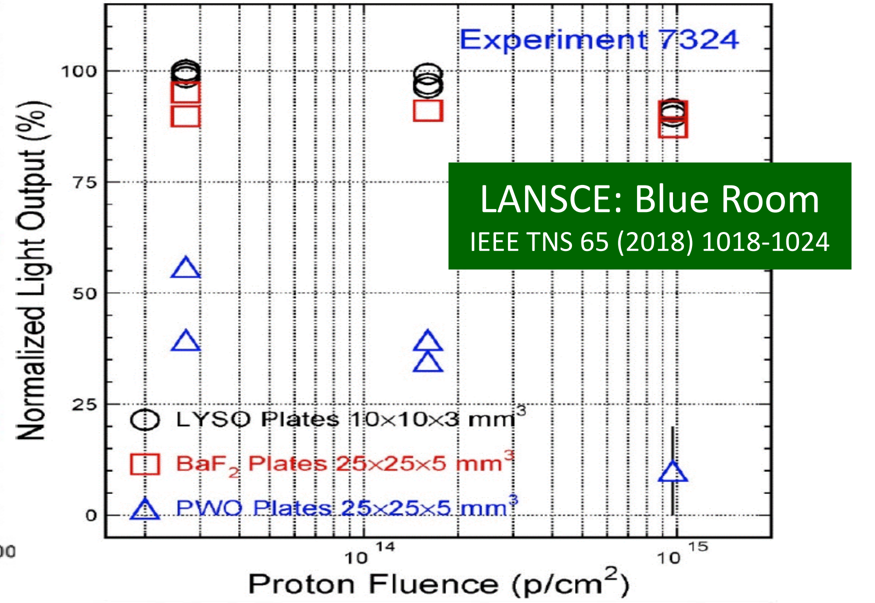

LANSCE: Blue Room
IEEE TNS 65 (2018) 1018-1024

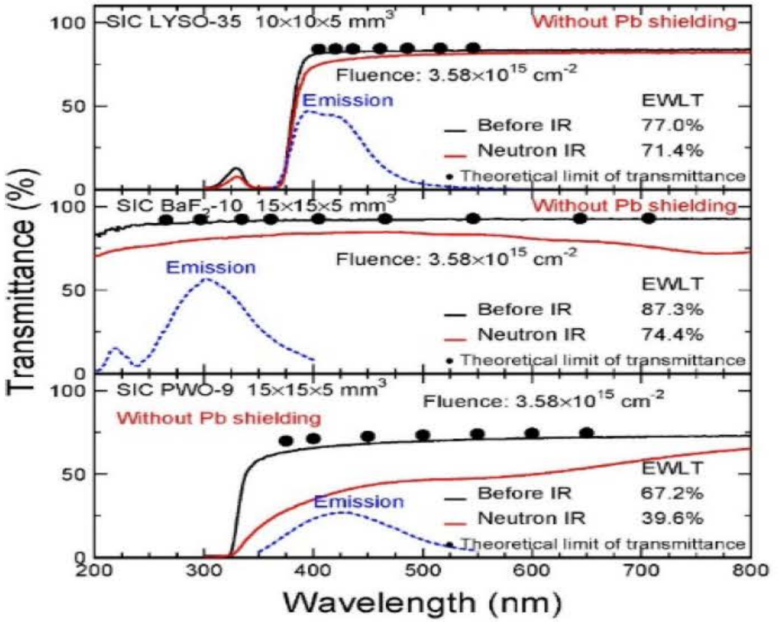

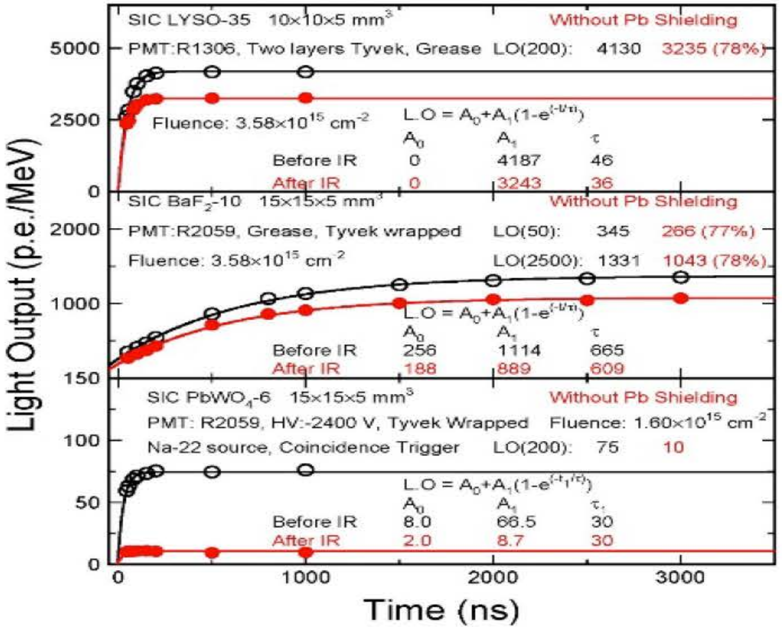

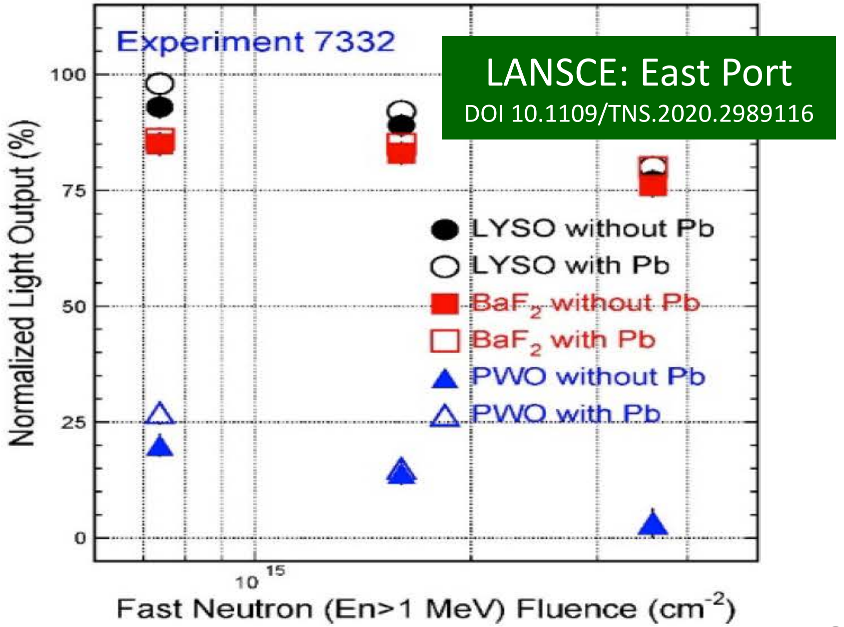

LANSCE: East Port
DOI 10.1109/TNS.2020.2989116

VUV PMT for BaF_2 and BaF_2:Y

Photo-detectors	$EWQE_{fast}$ (%)	$EWQE_{slow}$ (%)	BaF_2 LO_{fast}	BaF_2 LO_{slow}	BaF_2 F/S	BaF_2:Y LO_{fast}	BaF_2:Y LO_{slow}	BaF_2:Y F/S
Hamamatsu R2059	15.2	20.9	0.15	1.07	1/7.0	0.15	0.32	1/2.1
Photek solar blind PMT	25.6	10.6	0.26	0.54	1/2.1	0.25	0.15	1/0.6

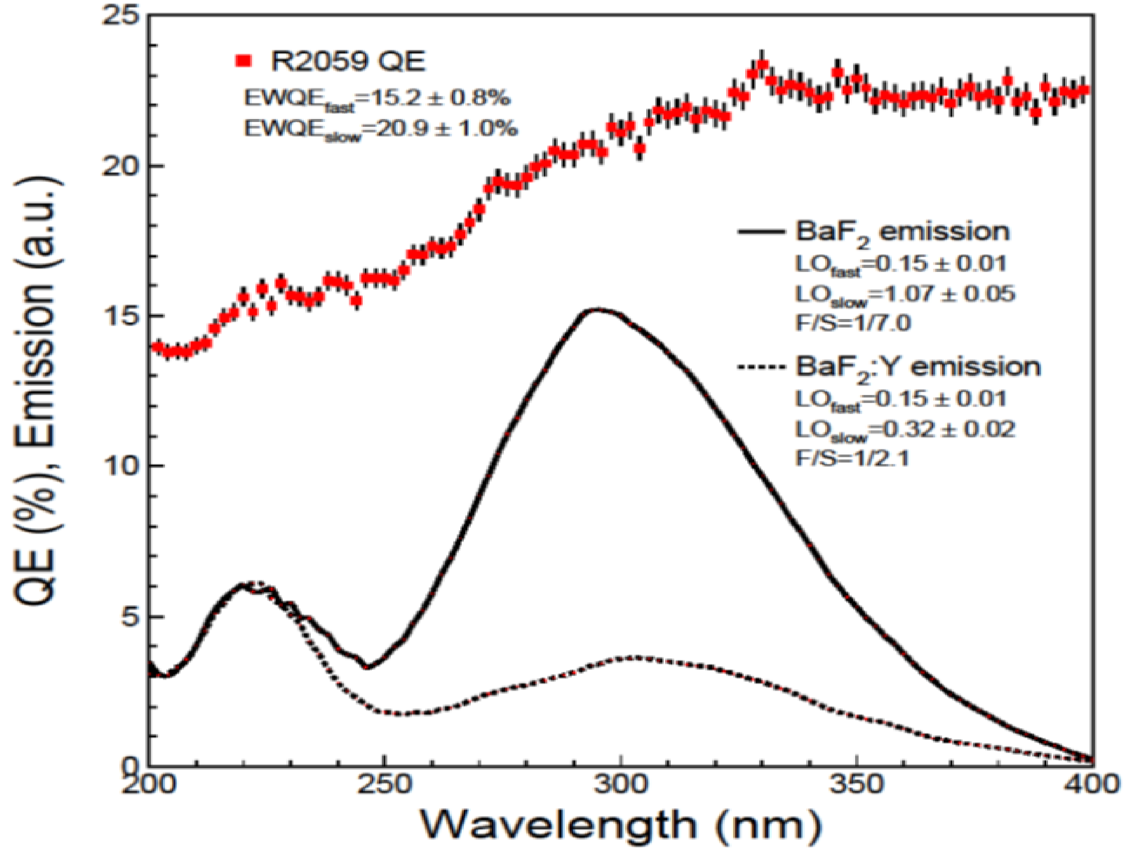

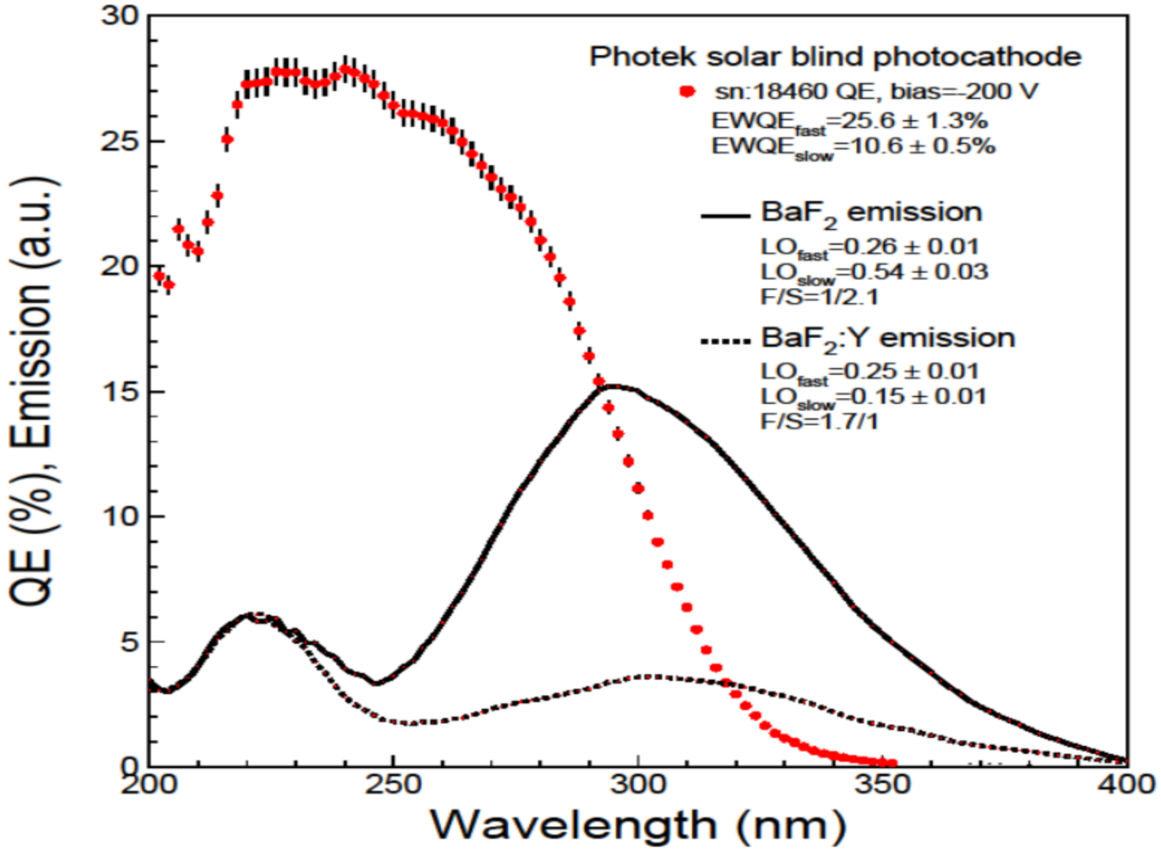

VUV SiPM for BaF_2 and BaF_2:Y

Photo-detectors	$EWQE_{fast}$ (%)	$EWQE_{slow}$ (%)	BaF_2 LO_{fast}	BaF_2 LO_{slow}	BaF_2 F/S	BaF_2:Y LO_{fast}	BaF_2:Y LO_{slow}	BaF_2:Y F/S
Hamamatsu s1337x	21.7	18.2	0.22	0.93	1/4.3	0.22	0.28	1/1.3
FBK-I SiPM	11.7	6.3	0.12	0.32	1/2.8	0.12	0.097	1/0.8

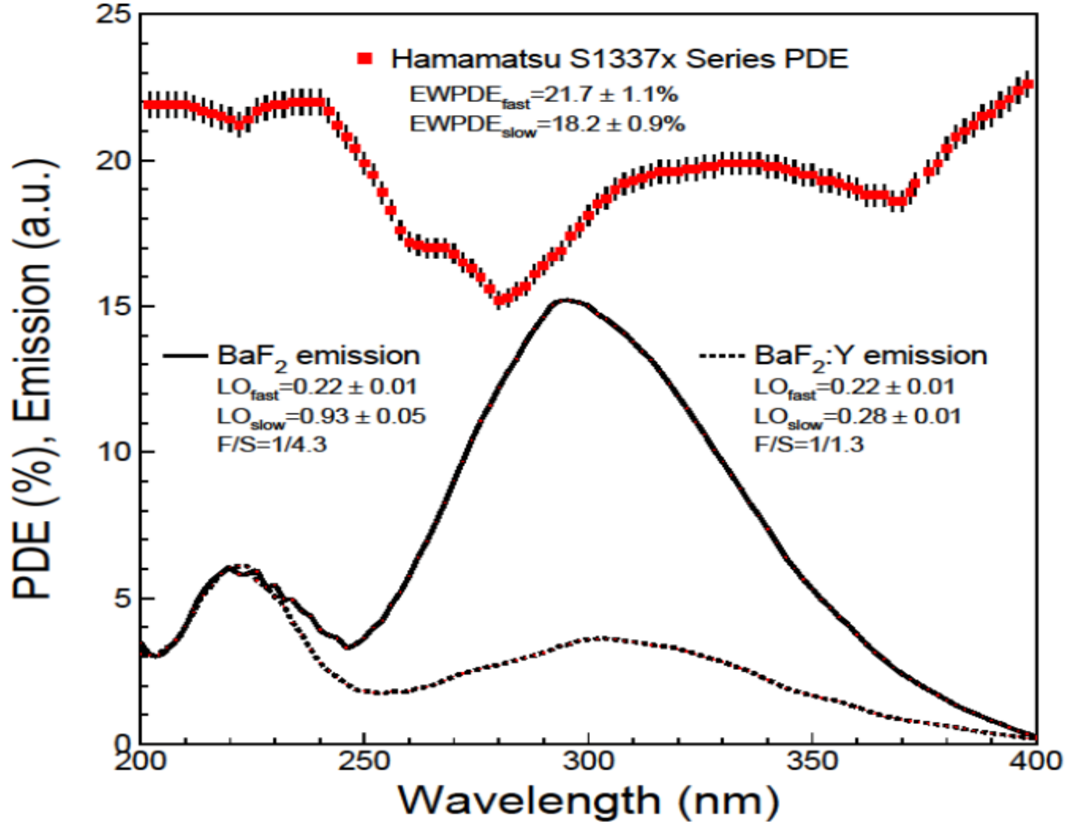

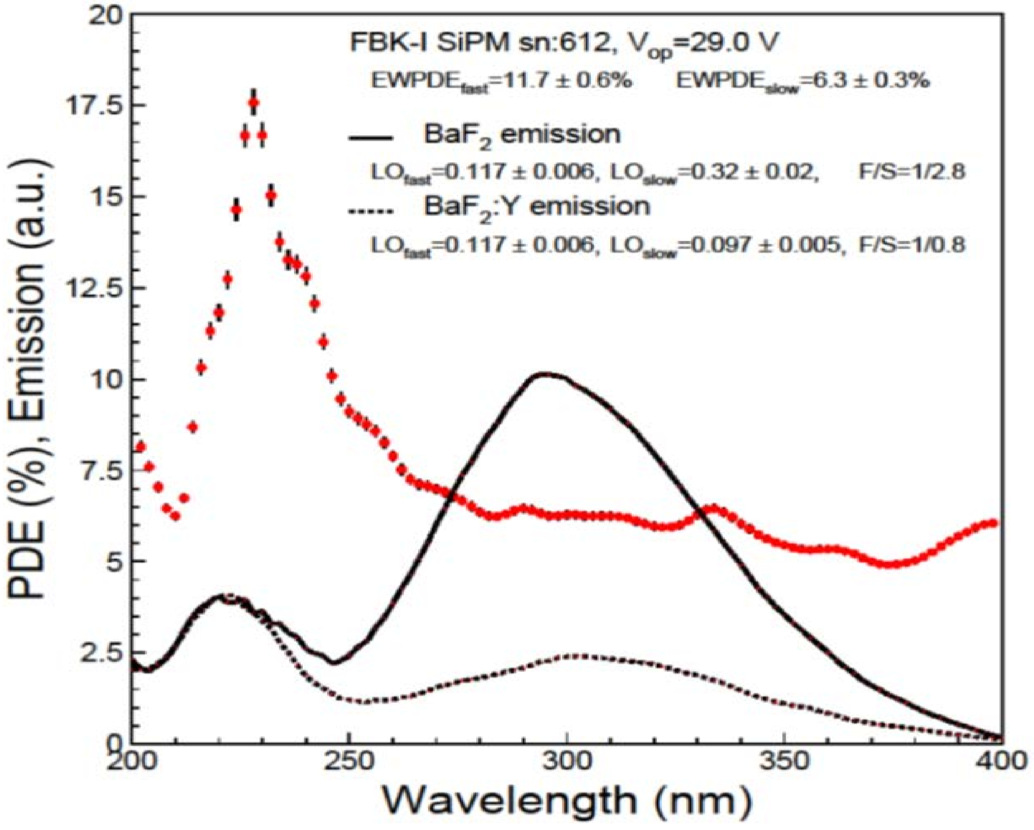

Homogeneous HCAL Concept

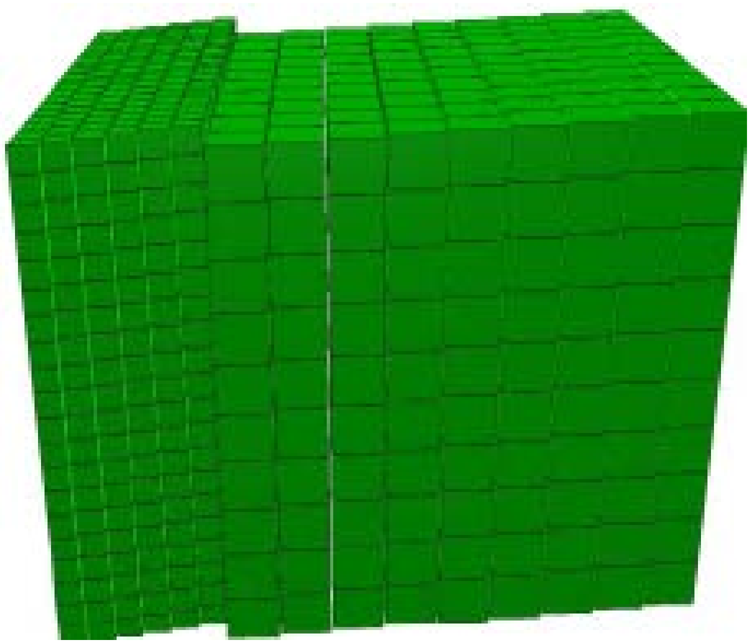

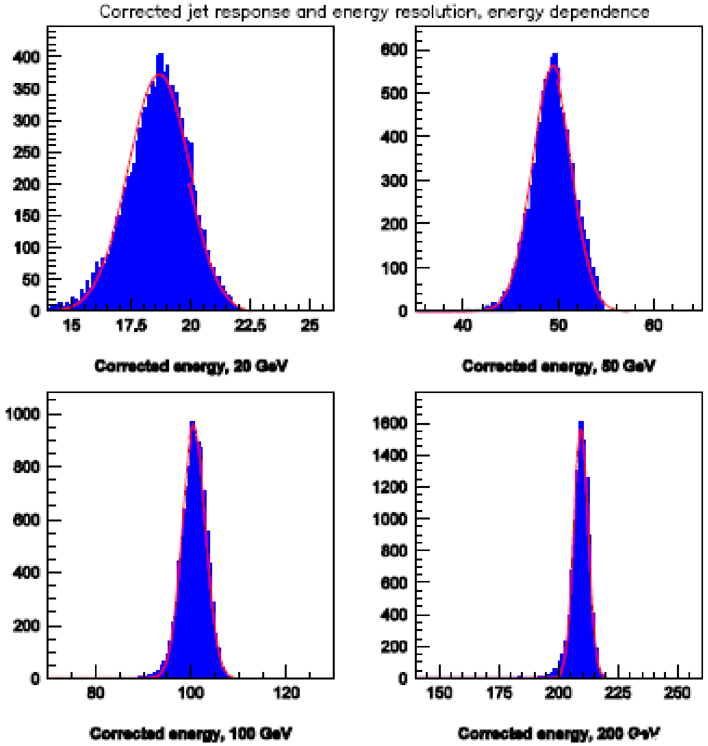

A. Para, H. Wenzel, and S. McGill in Callor2012 Proceedings and A. Benaglia *et al*., IEEE TNS **63** (2016) 574-579: a jet energy resolution at a level of 20%/√E by HHCAL with dual readout of S/C or dual gate

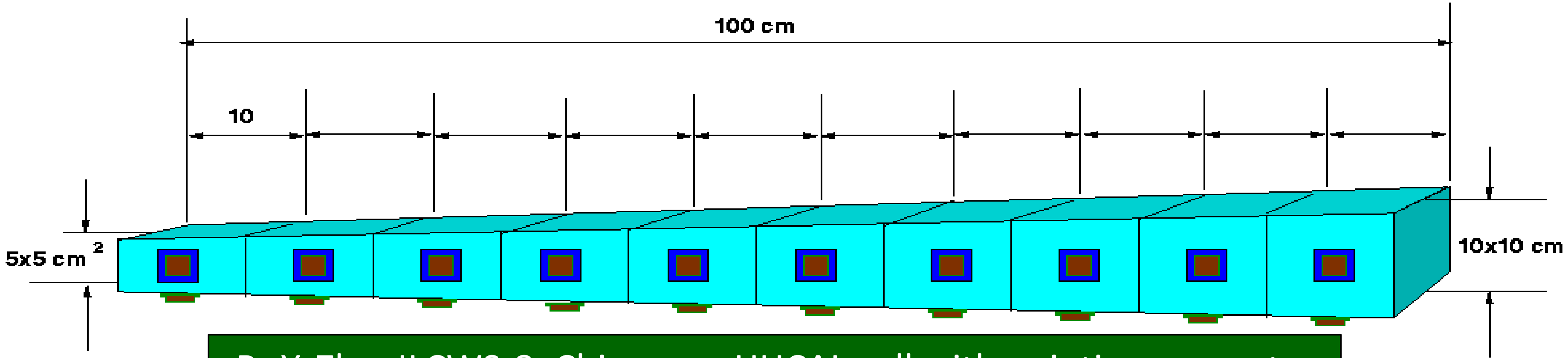

R.-Y. Zhu, ILCWS-8, Chicago: a HHCAL cell with pointing geometry

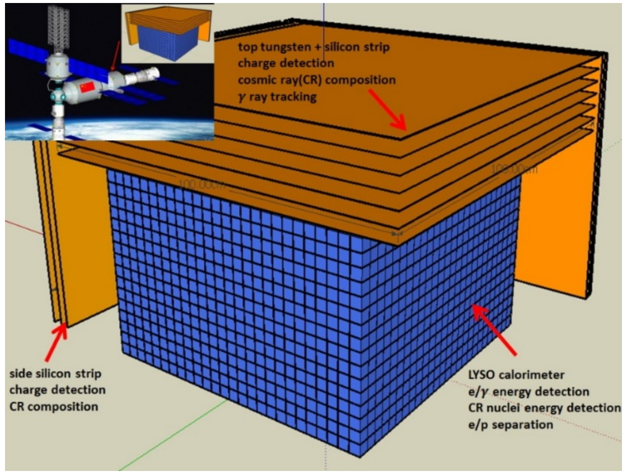

HERD LYSO Calorimeter in space

Can we afford?

Cost-Effective Sapphire Crystals for HHCAL

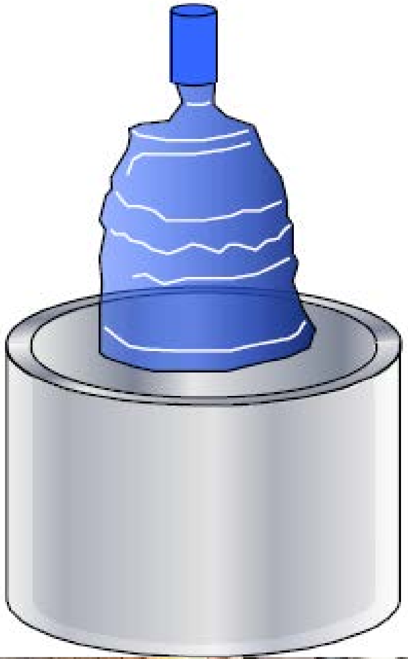

Prof. Xu Jun of Tongji University: Sapphire crystals by Kyropoulos (KY) technology
A producer can grow 1,000 tons ingots annually with 400 to 450 kg/ingot
Cost of mass-produced Sapphire crystals including processing: less than $1/cc

Sapphire Crystal	Weight (g)	Size (cm)	Unit Price	Comment
Ingot Boule	400,000	Φ50×55	US$12,000/pc	Undoped
Cutting/Polishing	4	1×1×1	**~US$0.6/cc**	Undoped

Sapphire:Ti Emission and Transmittance

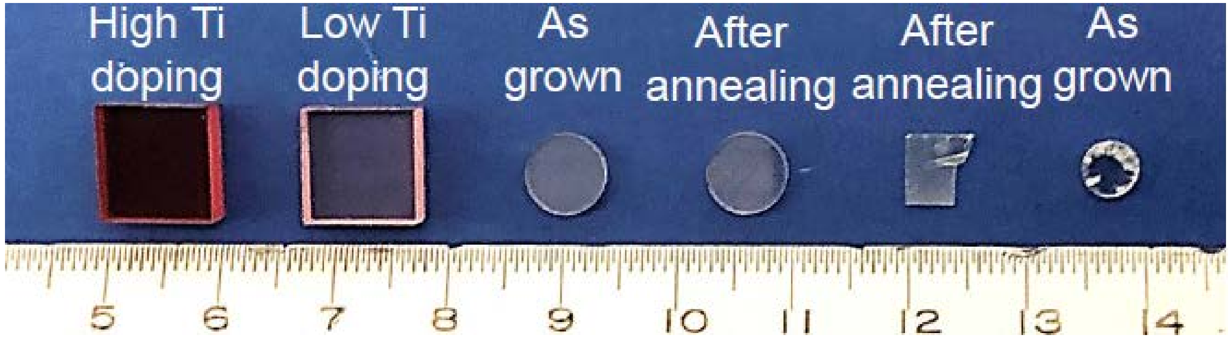

ID	Dimension (mm^3)	#	Polishing
Al_2O_3:Ti-1,2	**10×10×4**	**2**	**Two faces**
Al_2O_3:C-1,2	Φ7×1	2	Two faces
Lu_2O_3:Yb	6.4×4.8×0.4	1	Two faces
$LuScO_3$:Yb	Φ4.8×1.3	1	Two faces
All samples received on April 15st 2019 (Monday)			

A weak emission at 325 nm with 150 ns decay time
A strong emission at 755 nm with 3 μs decay time

Fast @325 nm

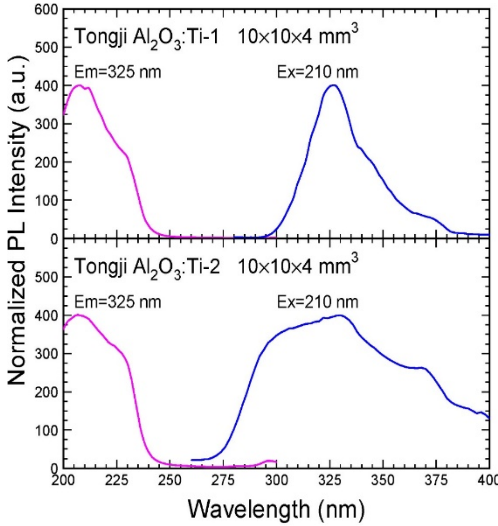

Slow @ 755 nm

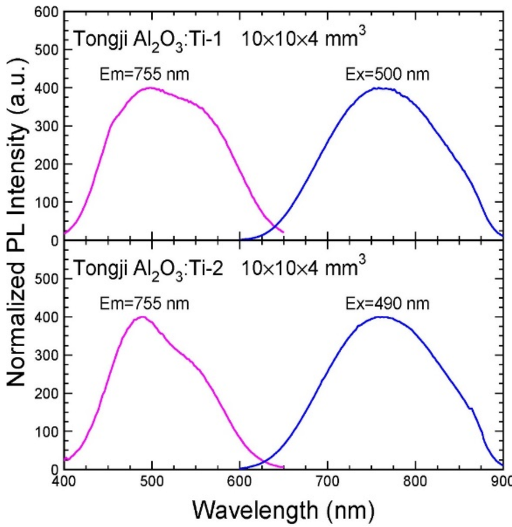

EWLT for Fast & Slow

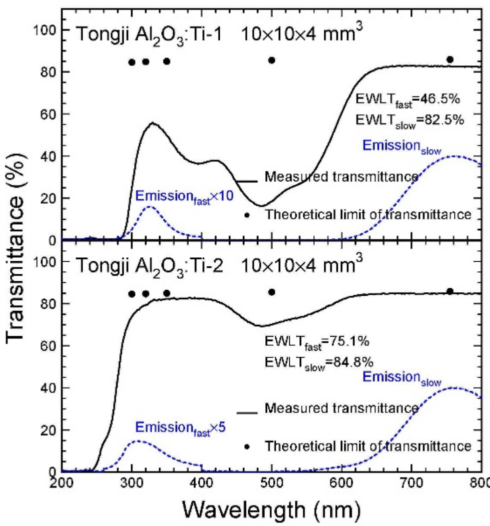

Fast Decay: 162 ns

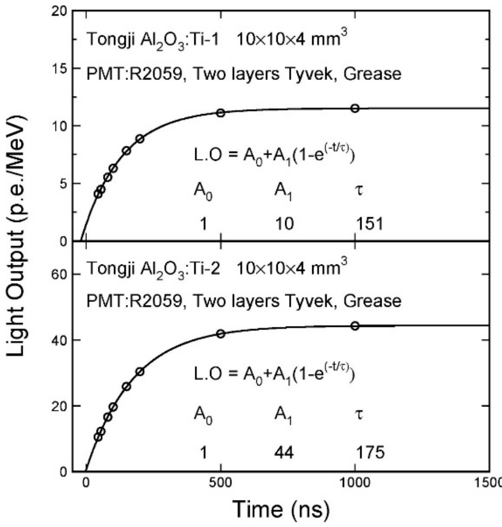

Slow Decay: 3.2 μs

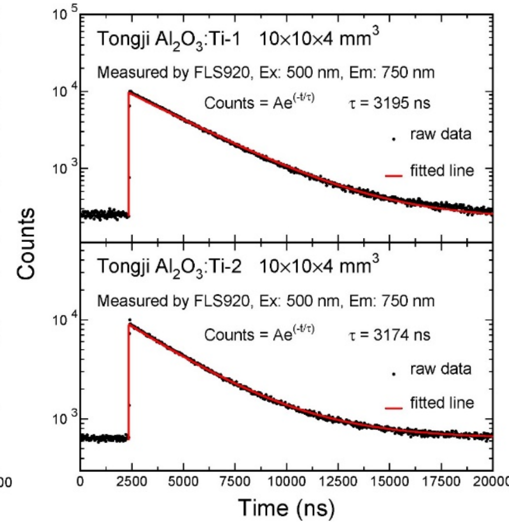

Light Output for Al_2O_3:Ti-1 and 2

Fast/slow component: 0.3k/6.4k and 1.3k/6.6k photons/MeV
Total: 6.7k and 7.9k photons/MeV, compatible with BGO

PHS: Al_2O_3:Ti-1/2

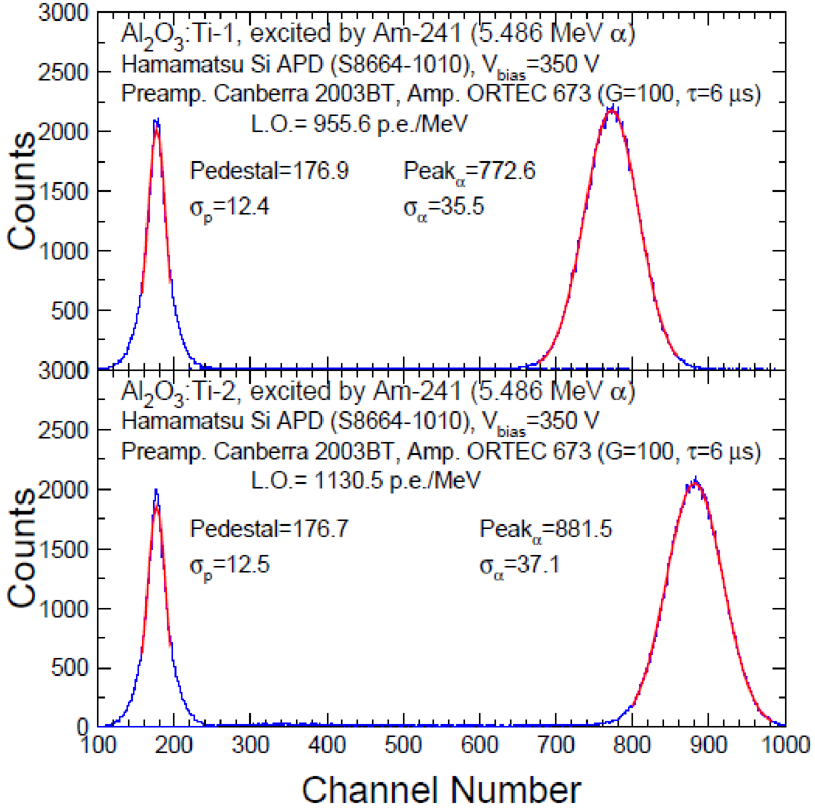

R2059 EWQE

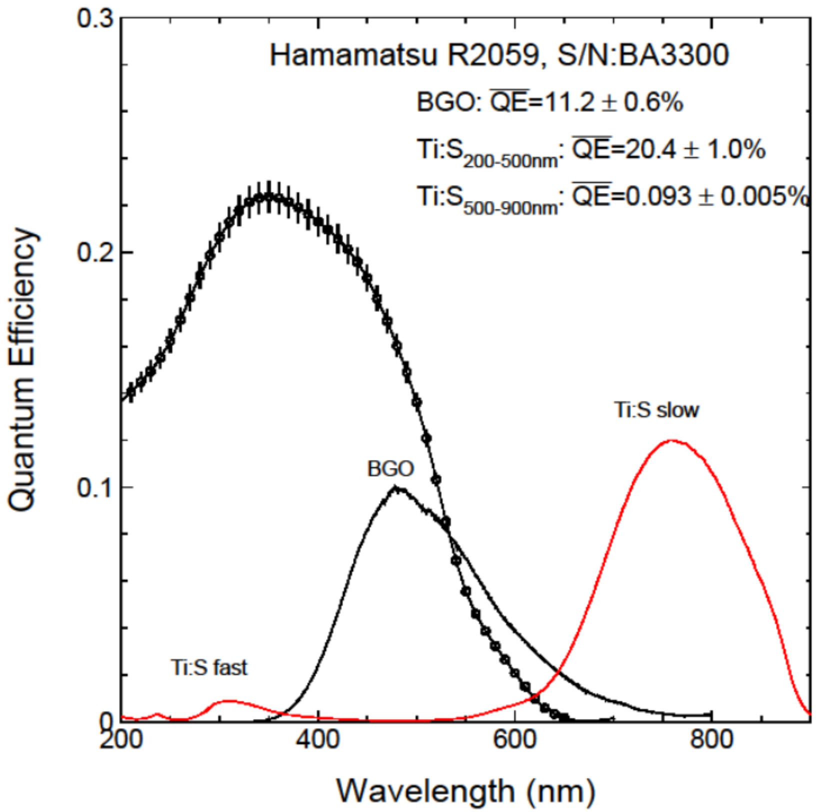

S6654-1010 EWQE

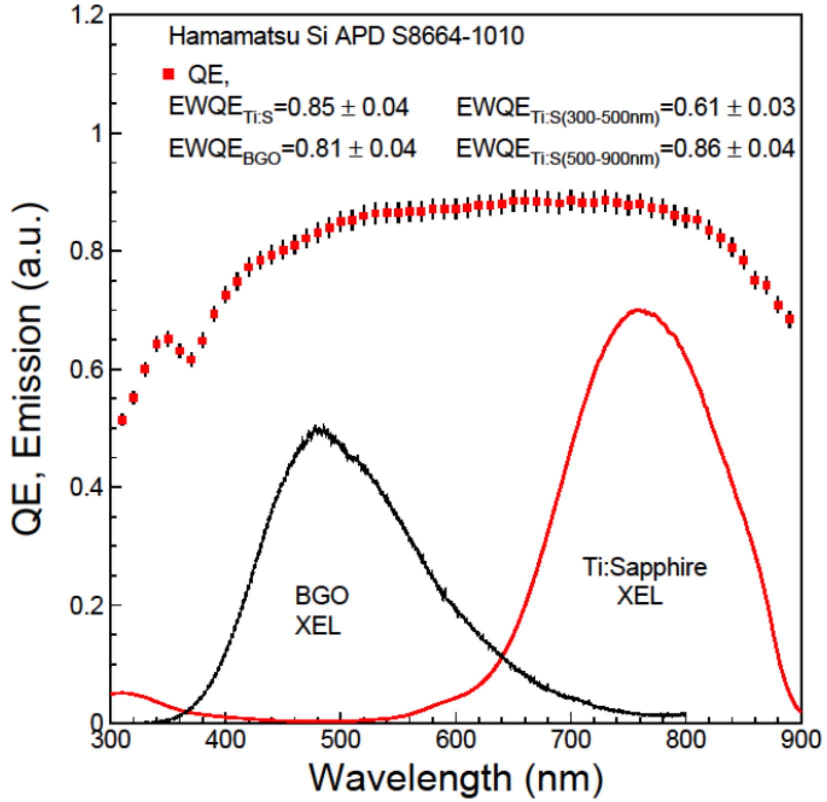

All Inorganic Cs Pb Halide Perovskite QD

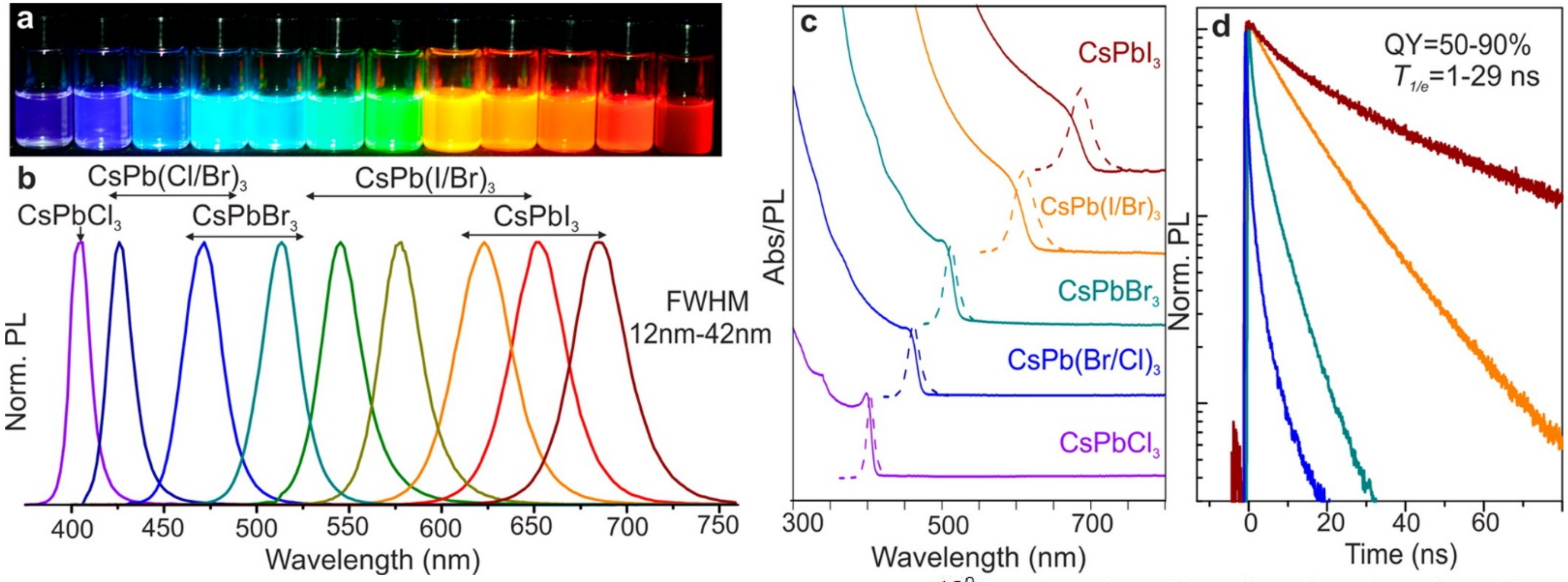

2015 | VOL 15 | Nano Lett. | 3692-3696

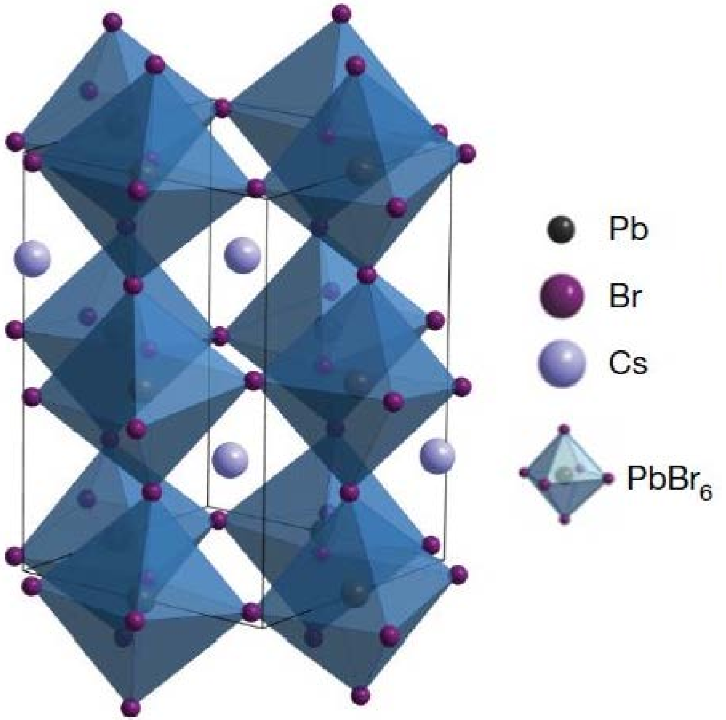

Absorption, emission wavelength and decay time can be tuned for size and composition with quantum efficiency up to 90%.

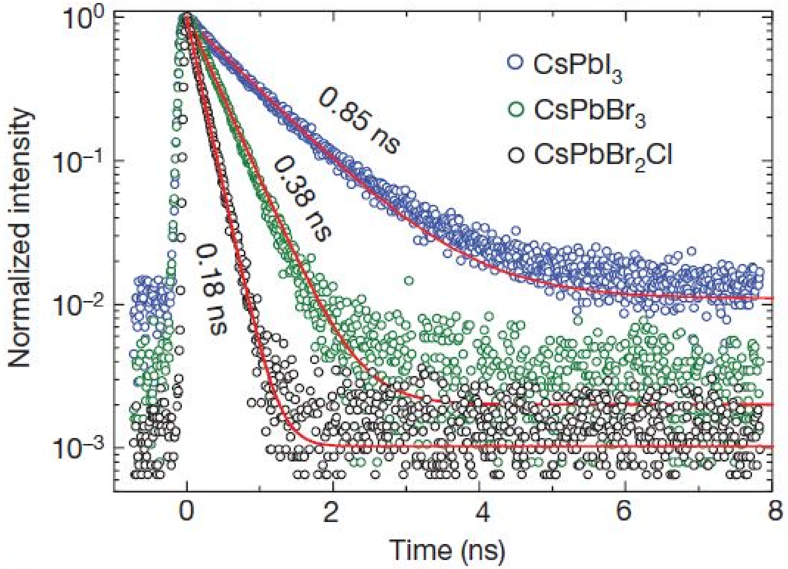

11 january 2018 | VOL 553 | Nature | 189

Summary

- LYSO crystals are radiation hard for HL-LHC applications, such as CMS BTL. BaF_2 shows a radiation hardness similar to LYSO at high radiation level. LuAG:Ce ceramics appears promising for FCC-hh, provided that its slow component is eliminated.
- Undoped BaF_2 crystals provide ultrafast light with sub-ns decay time. Yttrium doping enhances its F/S ratio while maintaining its sub-ns fast component not changed. 20 cm long BaF_2:Y crystals with LO_F>100 p.e./MeV, F/S>2, 10% LRU and $|\delta_F|<3\%/X_0$ are developed. R&D continues to optimize yttrium doping in large size BaF_2:Y crystals for Mu2e-II. SB photo-detectors are also under development for BaF_2:Y readout.
- Mass-produced Sapphire crystals costs less than $1/cc. Sapphire:Ti crystals show a weak/strong fast/slow scintillation at 325/755 nm with LO of 1.3k/6.6k photons/MeV and 151 ns/3 μs decay. With a cut-off of 280 nm and LO similar to BGO it may be used for an HHCAL with dual readout of both scintillation and Cerenkov light.
- Additional ultrafast scintillators under development, such as ZnO:Ga films, quantum confinement based all inorganic Cs Pb halide perovskite quantum dots etc.

Acknowledgements: DOE HEP Award DE-SC0011925

Diamond Photodetector

E. Monroy, F. Omnes and F. Calle,"Wide-bandgap semiconductor ultraviolet photodetectors, IOPscience 2003 Semicond. Sci. Technol. 18 R33

E. Pace and A. De Sio, "Innovative diamond photo-detectors for UV astrophysics", Mem. S.A.It. Suppl. Vol. 14, 84 (2010)

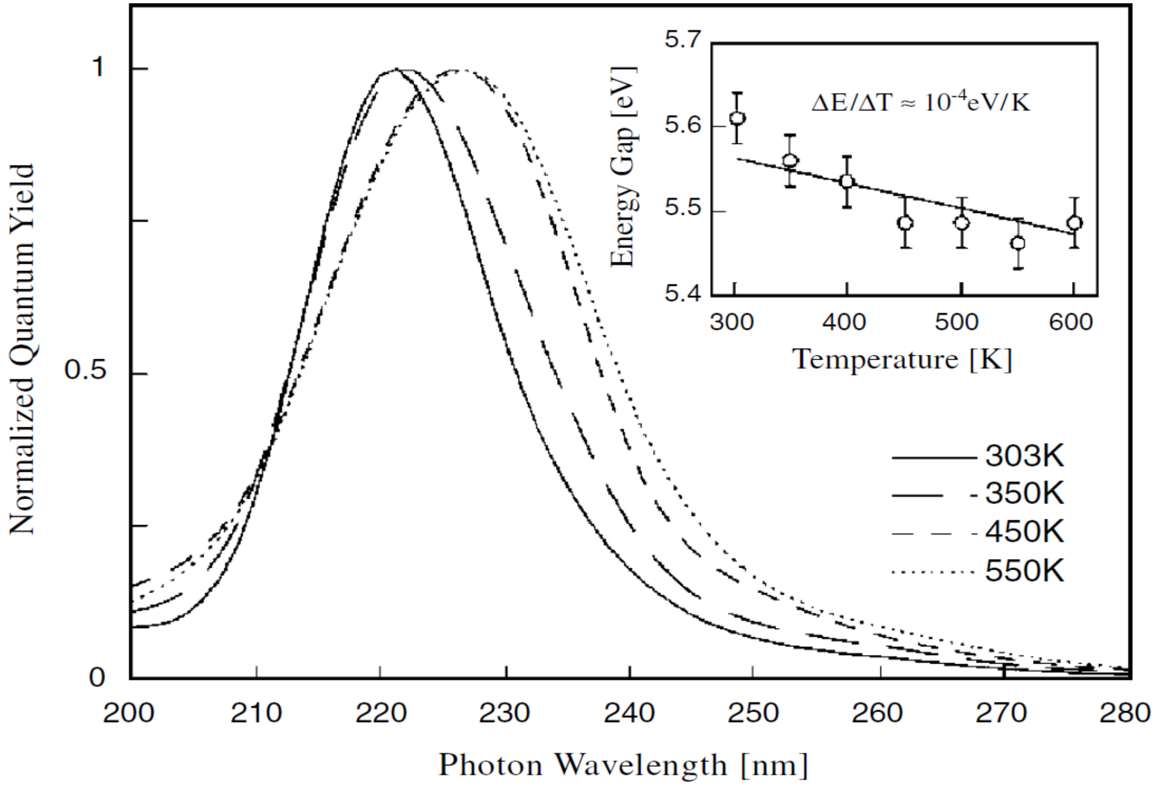

Figure 6. Quantum efficiency of diamond photoconductors at different temperatures and Arrhenius plot of the peak value (inset). (From [Sal00].)

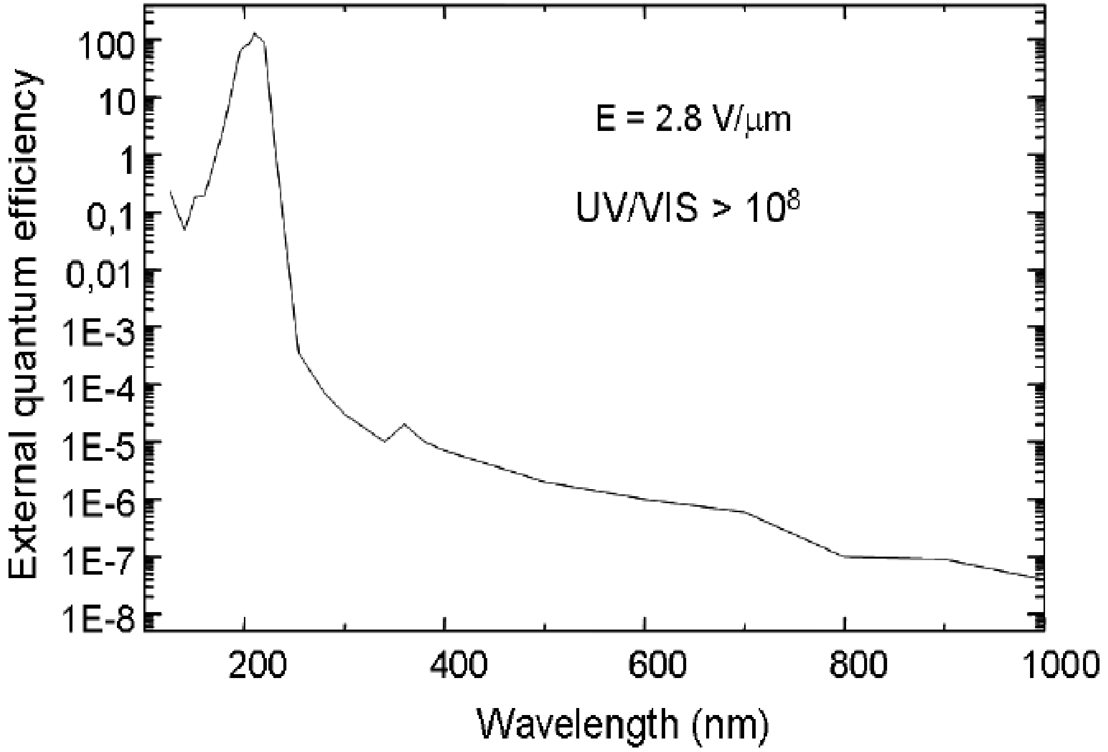

Fig. 4. External quantum efficiency extended to visible and near infrared wavelength regions. The